

AN EXPERIMENTAL STUDY ON OXIDATIVE COUPLING OF METHANE OVER  
Mn/Na<sub>2</sub>WO<sub>4</sub>/SiO<sub>2</sub> CATALYST

by

Yeşim DÜŞOVA

B.S., Chemical Engineering, Yıldız Technical University, 2009

Submitted to the Institute for Graduate Studies in  
Science and Engineering in partial fulfillment of  
the requirements for the degree of  
Master of Science

Graduate Program in Chemical Engineering

Boğaziçi University

2014

*to my family*

## ACKNOWLEDGEMENTS

Foremost, I would like to offer my truthful gratitude to my thesis supervisor Prof. Ramazan Yıldırım for his kindness, assistance and most of all, for his patience. I am very grateful to him for encouragement and far-sighted suggestions. He brings me different perspective during my research and keeps my interest and excitement on the project. It was also a privilege for me to work with my co-supervisor, Assoc. Prof. Ahmet Kerim Avcı. I am very grateful to his valuable advices. My sincere gratitude is due to my thesis committee members; Prof. Ahmet Erhan Aksoylu, Assoc. Prof. Abdullah Kerem Uğuz, Assoc. Prof. Hasan Bedir for spending their valuable time to read and comment on my thesis.

Very special thanks to Aybüke Leba and Melek Selcen Başar for their friendship, endless support and motivation. I feel very lucky to meet them. Heartfelt thanks to İrem Şen, her guidance and patience. I was very lucky to work with CATREL team, especially A. İpek Paksoy, Cansu Yassı, Elif Erdiç, Merve Eropak, Ali Uzun, Kerem Aksakal, Sinan Koç, Onur Kavaklı. I would like to thank to my friends in graduate class, Oya Gürsoy, Büşra Gürses, Özge Ertem, Didem Büşra Kabakçı. Their friendship and cheerfulness made my study so enjoyable. Special thanks to Sezin Sezen for helping and endless friendship during my thesis. Cordial thanks for Bilgi Dedeoğlu, Yakup Bal for their technical assistance, secretaries Melike Gürbüz and Belgin Balkan for their help.

Heartfelt thanks goes to my friends, Eda Burçak Dayı, Fulya Beteş, Merve Selek for all their support, friendship and encouragement throughout my life. I am very grateful to Selen Solak for her support and encouragement which has given me strength.

I am indebted to thank to my family for endless patience and unwavering belief in me; my sister for her cheerfulness; my grandparents for care and pray. Very special thanks to boundless of my mother who always supported my dreams. Her sacrifice and encouragement provides me to achieve my potential in everything I do. Lastly, my heartfelt thanks to my husband, Gökhan Teke, for his tireless encouragement and emotional support. This thesis would not been possible without them.

The financial support for this thesis was provided by TÜBİTAK through project 112M714.

## ABSTRACT

### AN EXPERIMENTAL STUDY ON OXIDATIVE COUPLING OF METHANE OVER Mn/Na<sub>2</sub>WO<sub>4</sub>/SiO<sub>2</sub> CATALYST

The oxidative coupling of methane (OCM) over Mn/Na<sub>2</sub>WO<sub>4</sub>/SiO<sub>2</sub> catalyst was investigated in this work. The 2wt%Mn/5wt%Na<sub>2</sub>WO<sub>4</sub>/SiO<sub>2</sub> catalysts were prepared using various methods (such as incipient to wetness impregnation, sol-gel and hydrothermal synthesis) and tested in a microflow quartz reactor for OCM process. Preliminary works were performed with 2wt.%Mn/5wt.%Na<sub>2</sub>WO<sub>4</sub>/SiO<sub>2</sub> particulate catalyst wall coated on the FeCrAl alloy plate replaced in a metal micro-channel reactor; the results were not satisfactory due to the weak adhesion of the silica support on the metal plate. Then the catalyst was wash-coated on a cordierite monolithic support resulting a better performance. In addition, the other catalytic structures such as particulate fixed beds, whole-structural rods (monosil) and mesoporous silica network (MCM-41) were also prepared and tested under various operating conditions (such as reactor filling material, operation temperature and feed composition). The reactor outlet stream was analyzed using gas chromatography to determine the CH<sub>4</sub> conversion and C<sub>2</sub> hydrocarbon selectivity. The highest yield (14.2%) was obtained using the particulate catalyst prepared by incipient to wetness impregnation method. The decreasing inside diameter of reactor from 10 mm to 2 mm after the catalyst bed, and filling the empty space with quartz chips significantly improved the catalytic performance. The highest C<sub>2</sub> yield was obtained at 650°C with CH<sub>4</sub>/O<sub>2</sub> ratio of 7.

## ÖZET

### **Mn/Na<sub>2</sub>WO<sub>4</sub>/SiO<sub>2</sub> KATALİZÖRÜ ÜZERİNDE METANIN OKSİJEN VARLIĞINDA YÜKSEK HİDROKARBONLU MOLEKÜLLERE DÖNÜŞÜMÜ**

Bu çalışmada metanın oksijen varlığında katalitik olarak etan ve etilene dönüştürülmesi (OCM) reaksiyonu Mn/Na<sub>2</sub>WO<sub>4</sub>/SiO<sub>2</sub> katalizörü kullanılarak incelenmiştir. Islak emdirme, sol-gel hazırlama ve hidrotermal sentez gibi çeşitli yöntemlerle hazırlanan 2wt.%Mn/5wt.%Na<sub>2</sub>WO<sub>4</sub>/SiO<sub>2</sub> katalizörünün OCM performansı mikro akışlı kuvars bir reaktör kullanılarak incelenmiştir. Çalışmalar öncelikle, katalizörün bir FeCrAl plaka yüzeyine kaplandığı metalik mikro kanal reaktörde başlamış ancak silika bazlı destek malzemesinin metal yüzeyine iyi yapışmamış olmasından dolayı performans düşük olmuştur. Sonra katalizör seramik monolitik mikro kanallara daldırma usulü ile kaplanmış, daha iyi sonuç alınmıştır. Buna ilave olarak, toz katalizörlerden oluşan sabit yatak, tek parça gözenekli çubuk (monosil) ve mezo gözenekli silika ağı (MCM-41) gibi yapılar da hazırlanmış, çeşitli reaksiyon koşullarında (çeşitli reaktör dolgu malzemesi, reaksiyon sıcaklığı ve besleme kompozisyonu) test edilmiştir. Reaktör çıkış akımı bir gaz kromatografi ile analiz edilerek CH<sub>4</sub> dönüşüm ve C<sub>2</sub> seçicilikleri belirlenmiştir. En yüksek verim (14.2%) ıslak emdirme yöntemi ile hazırlanan toz katalizör ile alınmıştır. Reaktör çapının katalizör sonrasında 10 mm'den 2 mm'ye düşürülmesi ve boşluğun kuvars parçacıkları ile doldurulması performansı önemli ölçüde artırmıştır. En yüksek C<sub>2</sub> verimi 650°C ile CH<sub>4</sub>/O<sub>2</sub> oranı 7 değerinde elde edilmiştir.

## TABLE OF CONTENT

ACKNOWLEDGEMENT .....	iv
ABSTRACT .....	vi
ÖZET .....	vii
LIST OF FIGURES .....	xi
LIST OF TABLES .....	xiv
LIST OF ACRONYMS/ABBREVIATIONS .....	xv
1. INTRODUCTION .....	1
2. LITERATURE SURVEY .....	3
2.1. Methane Utilization .....	3
2.2. Methods for Methane Utilization .....	4
2.2.1. Indirect Methods Utilization of Methane .....	5
2.2.2. Direct Methods for Methane Utilization .....	6
2.2.2.1. Oxidative Coupling of Methane to Higher Hydrocarbons .....	7
2.3. Methane Activation and Reaction Mechanisms .....	8
2.4. Catalysts for Oxidative Coupling of Methane .....	9
2.4.1. The Alkali and Alkali Earth Metal Oxide .....	10
2.4.2. Lanthanide and Actinide Metal Oxide .....	11
2.4.3. Transition Metal Oxides .....	12
2.5. Influences of Operating Conditions on the Oxidative Coupling of Methane Reaction .....	17
2.5.1. The effect of Feed Gas Composition .....	18
2.5.2. The effect of Reaction Temperature .....	18
2.5.3. The effect of Reactor Pressure .....	19
2.5.4. The effect of Residence Time .....	19
2.6. Types of Reactor Used for OCM .....	20
2.6.1. Microstructured Reactor .....	21
2.6.2. MonoSil Structured Reactors .....	23
2.7. Methods for Catalyst Preparation .....	26
2.7.1. Impregnation Method .....	26

2.7.2. Sol-gel Method of Catalyst Preparation .....	27
2.7.3. Monolithic Catalyst Preparation .....	29
3. EXPERIMENTAL WORK .....	32
3.1. Materials .....	32
3.1.1. Chemicals .....	32
3.1.2. Gases .....	34
3.2. Experimental Systems .....	34
3.2.1. Catalyst Preparation and Pretreatment .....	35
3.2.1.1. Particulate Catalyst Preparation with Impregnation Method .....	35
3.2.1.2. Particulate Catalyst Preparation with Sol-gel Method .....	37
3.2.1.3. Preparation and Pretreatment of Wall Coated Catalysts .....	38
3.2.1.4. Preparation and Pretreatment of Monolithic Support with Wash Coating .....	38
3.2.1.5. Monolithic Catalyst Preparation with Sol-gel Method .....	40
3.2.1.6. Preparation of Mn-MCM-41 Catalyst Support .....	41
3.2.2. Catalytic Reaction Tests for OCM Reaction .....	42
3.2.3. Product Analysis System for OCM Reaction .....	47
4. RESULTS AND DISCUSSIONS .....	49
4.1. Preliminary Work .....	49
4.1.1. Experimental Results on the Coated Catalyst Layer on the FeCrAl Alloy Plate .....	49
4.1.2. Experimental Results on the Catalyst Coated on the Cordierite Monolithic Support .....	50
4.2. Design of the Reactor .....	52
4.2.1. Reactor Tube Diameter .....	52
4.2.2. Reactor Filling Material .....	52
4.3. Effects of Catalyst Preparation and Operational Conditions .....	54
4.3.1. Effects of Operational Conditions .....	54
4.3.2. Experiments with Different Catalysts Forms .....	57
5. CONCLUSIONS AND RECOMMENDATIONS .....	63
5.1. Conclusions .....	63
5.2. Recommendations .....	64
APPENDIX A: CALIBRATION CURVES OF MASS FLOW CONTROLLERS .....	65

REFERENCES ..... 69

## LIST OF FIGURES

Figure 2.1.	Geographical distribution of proven natural gas reserves, (BP Statistic Review of World Energy, 2011). .....	4
Figure 2.2.	Methods for methane utilization from natural gas. ....	5
Figure 2.3.	Reaction mechanism for the oxidative coupling of methane (Lee <i>et al.</i> , 2012). .....	9
Figure 2.4.	Two tentative models involving the possible formation of active oxygen species (O*). .....	15
Figure 2.5.	Figure 2.5. The form and pore size distribution of the MonoSil (a) Prepared MonoSil, (b) Monosil as a microrreactor, (c) SEM images, (d) Flow through pores and (e) Struts (Kadib <i>et al.</i> , 2009). .....	25
Figure 2.6.	The monolithic structure used in the experiments. ....	30
Figure 2.7.	Schematic diagram of a monolith structure (Tomašić and Jović, 2006). ..	31
Figure 3.1.	Schematic diagram of the impregnation system (a) Ultrasonic mixer, (b) Büchner flask, (c) Vacuum pump, (d) Peristaltic pump, (e) Reactant storage tank and (f) Silicone tubing. ....	36
Figure 3.2.	Schematic diagram of the sol-gel system (a) pH meter, (b) Heater and (c) Thermometer. ....	37
Figure 3.3.	The monolith coating system (a) Dipping Procedure in Ultrasonic mixer, (b) Compressed Air Flow and (c) Microwave Oven. ....	39

Figure 3.4.	Preparation of Monolithic catalyst (Monosil) with sol-gel method (a) Preparation step, (b) Aging in the oven, (c) and (d) Monolithic catalyst (Monosil). .....	41
Figure 3.5.	Synthesis process of MCM-41. ....	42
Figure 3.6.	The microreactor flow system and product analysis system. ....	44
Figure 3.7.	10 mm and 10 to 2 mm narrower ID quartz fixed-bed down flow reactor. ....	45
Figure 3.8.	Top (at the left) and cross-sectional (at the right) view of the coated microchannel configuration; (a) Engineered metal housing, (b) Open microchannels, (c) Coated catalyst layer, (d) FeCrAl alloy plate and (e) Ceramic wool plug (Şimşek, 2012). ....	46
Figure 3.9.	Quartz tube reactor filled with quartz chips (a) Whole reactor, (b) Particulate catalyst, (c) Particulate catalyst (crushed monolithic particulate) and (d) Cordierite monoliths. ....	47
Figure 4.1.	Results of the experiments of comparison of the coated catalyst layer with the 20wt.% $\alpha$ -Al <sub>2</sub> O <sub>3</sub> included catalyst coated layer. ....	50
Figure 4.2.	Effect of using cordierite monolithic support with different coating methods. ....	51
Figure 4.3.	Effect of using different kinds of filling material. ....	54
Figure 4.4.	Effect of reaction temperature on the CH <sub>4</sub> conversion and C <sub>2</sub> selectivity, CH <sub>4</sub> /O <sub>2</sub> ratio is 7. ....	55
Figure 4.5.	Effect of CH <sub>4</sub> /O <sub>2</sub> ratio on the CH <sub>4</sub> conversion at different temperature. ..	56

Figure 4.6.	Effect of CH <sub>4</sub> /O <sub>2</sub> ratio on the C <sub>2</sub> selectivity at different temperature. ...	57
Figure 4.7.	Various types of catalysts prepared via different methods. ....	58
Figure 4.8.	Comparasion of the catalysts that are prepared by different methods (Reaction temperature at 700°C, CH <sub>4</sub> /O <sub>2</sub> ratio is 10). ....	62
Figure A.1.	MFC calibration curve for ethylene. ....	65
Figure A.2.	MFC calibration curve for methane. ....	65
Figure A.3.	MFC calibration curve for ethane. ....	66
Figure A.4.	MFC calibration curve for oxygen. ....	66
Figure A.5.	MFC calibration curve for helium. ....	67
Figure A.6.	MFC calibration curve for hydrogen. ....	67
Figure A.7.	MFC calibration curve for mixture (5% methane, 2% ethane, 2% ethylene, 81% helium). ....	68

## LIST OF TABLES

Table 3.1.	Chemicals used in catalyst preparation (all specifications: research grade). .....	32
Table 3.2.	Specifications and applications of the gases used in the study. ....	34
Table 3.3.	Reactant and product gas analysis conditions. ....	48
Table 4.1.	Particulate catalyst* performance at temperature 650 and 700°C, CH <sub>4</sub> /O <sub>2</sub> ratio 7 and 10. ....	59
Table 4.2.	Particulate catalyst* performance at temperature 650 and 700°C, CH <sub>4</sub> /O <sub>2</sub> ratio 7 and 10. ....	59
Table 4.3.	Monosil catalyst* performance at temperature 650 and 700°C, CH <sub>4</sub> /O <sub>2</sub> ratio 7 and 10. ....	60
Table 4.4.	Monosil catalyst* performance at temperature 650 and 700°C, CH <sub>4</sub> /O <sub>2</sub> ratio 7 and 10. ....	60
Table 4.5.	MCM-41 catalyst performance at temperature 650 and 700°C, CH <sub>4</sub> /O <sub>2</sub> ratio 7 and 10. ....	61
Table 4.6.	Comparasion of the catalysts that are prepared by different methods (Reaction temperature at 700°C, CH <sub>4</sub> /O <sub>2</sub> ratio is 10). ....	61

## LIST OF ACRONYMS/ABBREVIATIONS

BOS	Birleşik Oksijen Sanayi
CTMABr	Cetyltrimethylammonium Bromide
CVD	Chemical Vapor Deposition
GHSV	High Residence Times for The Gas
HPLC	High Performance Liquid Chromatography
IW	Incipient to Wetness Impregnation Method
OCM	Oxidative Coupling of Methane
PEG	Poly-ethylene Glycol
PVC	Polyvinyl Chloride
PVD	Physical Vapor Deposition
POX	Partial Oxidation Reforming
RTD	Residence Time Distribution
SR	Steam Reforming
TCD	Thermal Conductivity Detector
TEOS	Tetraethylorthosilicate
TMOS	Tetramethylorthosilicate
WGS	Water-Gas Shift Reaction

## 1. INTRODUCTION

Natural gas can be utilized as an alternative feedstock for the chemical industry since a huge untapped natural gas reserves exist (more than oil). The petroleum refining and petrochemical processes can also supply remarkable amount of methane. The conversion of natural gas to higher hydrocarbons provides easy purification (Shebdelfar *et al.*, 2012). Near future prediction is expected a decline in oil production as natural gas received great attention as a source of energy and organic carbon (Choudhary and Uphade, 2004). On the other hand, its uneconomical transportation causes that the methane to be let out or flared in the remote places, creating another serious problem: the methane and carbon are the most significant greenhouse gases responsible for global warming. Hence increasing energy cost and environmental problems will make worthwhile of the conversion of natural gas to more valuable products such as ethylene which is a feedstock for petrochemical industry (Lunsford, 2000).

Oxidative coupling of methane (OCM) transform methane to C<sub>2</sub> hydrocarbons (ethane and ethylene) is a promising source of more valuable chemicals for petrochemical industries. OCM is considered as an alternative technology in direct methane conversion to overcome the lack of energy and resource wasting indirect conversion processes (Stünkel *et al.*, 2008). The challenge of the process delaying the commercialization is the low C<sub>2</sub> yield (Shebdelfar *et al.*, 2012).

OCM generally occurs under high temperature 600-800°C because of the extremely high stability of the C-H bonds in CH<sub>4</sub> molecule and affected the unselective gas phase radical reactions due to the deep oxidation of C<sub>2</sub> products to CO<sub>x</sub> (Wolf, 1992). The process let to produce desired products that are more reactive than methane and achieve high selectivity at only low conversion of methane. The process requires high thermal and hydrothermal stability catalyst to avoid catalyst deactivation during high-temperature catalyst calcinations and reaction. This leads to a trouble to develop a commercial catalyst for the OCM reaction (Choudhary and Uphade, 2004).

Another challenge of the OCM process is the separation of product steam that involves low concentration of ethylene increasing the cost of separation (Choudhary and Uphade, 2004).

For the development of an effective OCM process, the catalysts tested in the literature are usually the metal oxides, which can be separated into three groups: the alkali and alkali earth metal oxide, lanthanide and actinide metal oxide and transition metal oxides. Some catalysts are enriched with active metals such as Mn and  $\text{Na}_2\text{WO}_4$  to improve the selectivity and effectiveness of the catalyst. High specific surface area and porosity of the catalyst are the important properties determining the preparation methods and thermal treatments for the effective catalyst.

The objective of this study was to develop and test a suitable micro-structured reaction system using silica supported Mn and  $\text{Na}_2\text{WO}_4$  catalyst to conversion of methane to ethane and ethylene. The reactions were performed using a micro-flow quartz tube reactor in four basic structures: particulate fixed bed, wall coated in metal microchannel, wash coat monoliths and single monolithic structures. Three different methods (incipient to wetness to impregnation method, sol-gel method and direct hydrothermal synthesis method (MCM-41)) are applied to synthesize the catalyst. The catalyst contents of the active metal remains 2wt.%Mn and 5wt.% $\text{Na}_2\text{WO}_4$  the same all the preparation ways. The reaction temperature and  $\text{CH}_4/\text{O}_2$  feed composition was investigated with the particulate catalyst synthesized by incipient to wetness impregnation.

Chapter 2 includes the literature survey on oxidative coupling of methane process, catalysts, influence of the operating conditions (feed gas composition, temperature and pressure and residence time) on the reaction performance, types of reactor and methods for catalyst preparation. The experimental system and catalyst preparation methods used and all experimental works are carried out in this study are detailed in Chapter 3. The experimental results are presented and discussed in Chapter 4; whereas Chapter 5 includes conclusion of the experimental study and recommendation for the future work.

## 2. LITERATURE SURVEY

Continuously expanding trend in the world is to reduce environmental pollutions, capital and operating costs of processes while to increase the efficiency, all of which involve reducing the energy consumption. To achieve this, there is a strong incentive to develop new processes for production of fuels and chemicals, and the methane utilization is one of the most studied for this purpose.

### 2.1. Methane Utilization

Natural gas, containing primarily (60-90%) methane, has been widely used as a feedstock for the production of more valuable chemicals and energy, and it seems to continue to be significant source of energy well into the 21<sup>st</sup> century. Potential reserves are abundant (at least 200 trillion m<sup>3</sup> worldwide (Alvarez-Galvan *et al.*, 2011); it is estimated that stranded reserves makes up 30% of natural gas reserves.

Methane is an excellent raw material to be converted into more valuable chemicals such as methanol, formaldehyde, syngas, liquid fuels and ethylene. Methane is an ideal fuel for home and industrial heating as well as for generation of electrical power because it is easy to remove sulfur compounds via purification (Holmen *et al.*, 2009). It has the largest heat of combustion between the hydrocarbons per unit of CO<sub>2</sub> formed. However, the known reserve of methane, which is comparable with liquid petroleum, is enormously underutilized as the source for chemicals (Lunsford, 2000).

The geographical distribution of natural gas (methane) shows in Figure 2.1; more than 70% known resources are located in remote areas and far away from the industrial plants, the off-shore use for production or transportation with pipelines are not feasible solutions for medium and smaller scale of gas fields. On the other hand, expensive liquefaction process for shipping from the ocean by vessels is another economic challenge (environmental catalysis). In addition, approximately 11% of the gas was re-injected while another 4% is vented or flared increasing the environmental challenge as in the form of

waste of energy and contribution to greenhouse gas emission (Lunsford, 2000; Rahimpour *et al.*, 2011).

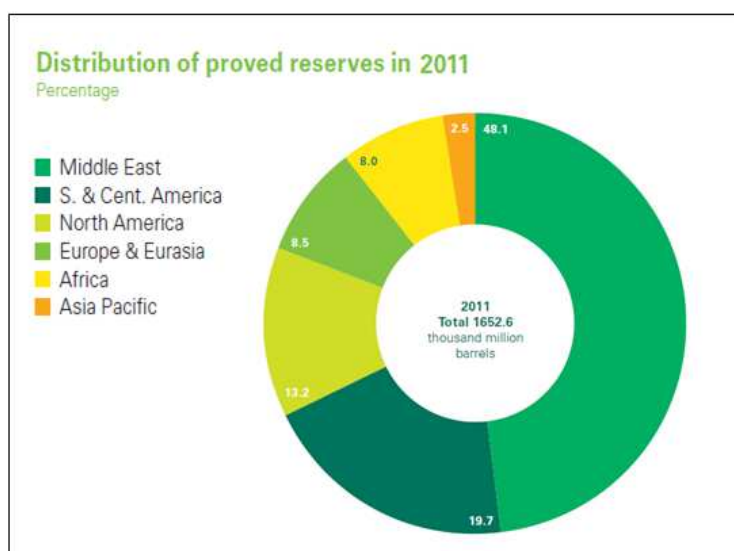


Figure 2.1. Geographical distribution of proven natural gas reserves (adapted from BP Statistical Review of World Energy, 2011).

## 2.2. Methods for Methane Utilization

The predominant component of natural gas is methane, which is very stable with the highest C-H bond ( $\Delta(\text{C-H}) = 438.8 \text{ kJ mol}^{-1}$ ) strength of all alkenes; this explains why it is found such in huge resources under the earth. Its activation energy is so high that it requires high temperature or use of oxidations agents to split the C-H bonds. It has high ionization potential (12.5eV), low proton affinity (4.4eV) and low acidity ( $\text{pK}_a=42$ ) and contains no functional group to facilitate chemical attacks.

Catalytic conversion of methane has been studied in two (direct and indirect) routes (Figure 2.2). The indirect routes on the production of syngas ( $\text{H}_2$  and CO mixture) in presence of water (steam reforming),  $\text{CO}_2$  (carbon dioxide reforming) or oxygen (partial oxidation). Then the Fischer Tropsch process converts the synthesis gas to the higher hydrocarbons (Akin and Lin, 2002). The direct methods for the conversion of methane, which aim to circumvent the highly energy intensive step of synthesis gas formation, are

partial oxidation to methanol and oxidative coupling of methane to hydrocarbons. The direct methods are considered potentially more economical and energy efficient because more than 60% of the capital cost of the Fischer Tropsch plants is related to the steam reforming. On the other hand, the direct processes have not yet advanced to a commercial stage (Vasireddy *et al.*, 2010).

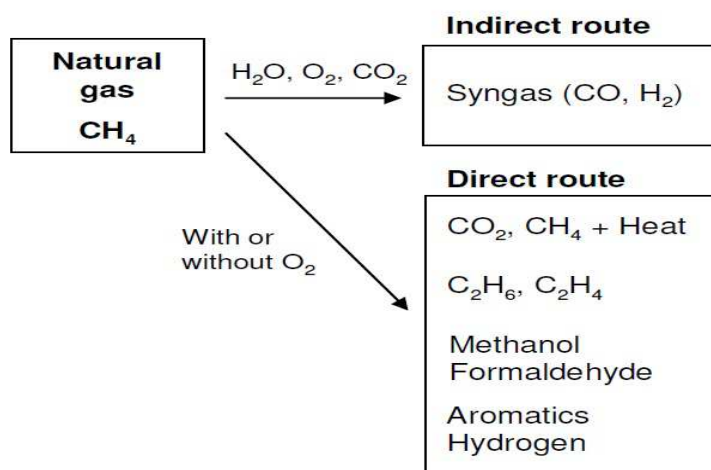
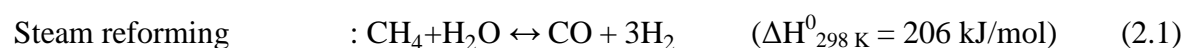


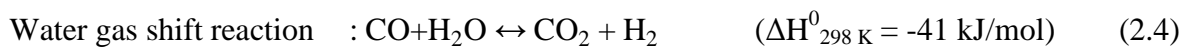
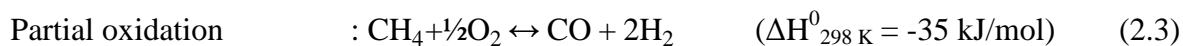
Figure 2.2. Methods for methane utilization from natural gas.

Direct or indirect processes require the use of oxygen, which is nearly as costly as methane. Hence the possibility of producing aromatics such as benzene, toluene and naphthalene by having methane reacted with hydrogen without an oxidant is also investigated (Ji *et al.*, 2002).

### 2.2.1. Indirect Methods Utilization of Methane

The synthesis gas, which contains carbon monoxide and hydrogen, is obtained from various feedstock and processes; it can be produced by steam reforming or (catalytic) partial oxidation of fossil fuels such as coal, natural gas, refinery residues. The current technologies for the production of synthesis gas are widely used to generate syngas with a stoichiometric ratio of hydrogen and carbon monoxide. The most important reactions are:





Methane reforming reactions are highly endothermic and only the one using steam does not require oxygen (Onsan, 2007). However the requirements of considerable heat input and high catalyst loadings make them unlikely to be used for hydrogen generation. By contrast, partial oxidation is slightly exothermic, but requires oxygen or air. Partial oxidation process converts hydrocarbons into hydrogen by partially combusting the hydrocarbon with oxygen. POX contains two parts that is reforming of the remaining  $\text{CH}_4$  with  $\text{O}_2$  and  $\text{CO}_2$  which comes after total combustion of  $\text{CH}_4$  over most catalysts. These two steps (total combustion and reforming) can be broken down in a process officially known as auto thermal reforming (Lunsford, 2000). Water gas shift reaction provides a complement to these three methods for synthesis gas formation. At a fundamental level, the WGS occurs simultaneously with SR and POX reactions.

### 2.2.2. Direct Methods for Methane Utilization

Many methods have been investigated for improving the industrial processes to convert methane into olefins and higher hydrocarbons to eliminate the expensive separation steps and high temperatures above  $600^\circ\text{C}$  with the corresponding high energy consumption. Additionally, direct methane conversion obviates the requirement of the system while provides to improve the economy of the process (Alvarez *et al.*, 2011). Both kinetics and unfavorable thermodynamic problems are associated with the direct conversion of methane without strong oxidant. It is difficult to activate the strong C-H bond, which makes the possible products more reactive than methane; this means that the challenge in methane conversion is related to selectivity rather than reactivity (Holmen *et al.*, 2009). Otherwise direct methods of methane conversion have distinct economic advantage over indirect methods in order to circumvent the expensive syngas step (Lunsford, 2000). Some of the direct approaches for methane utilization are:

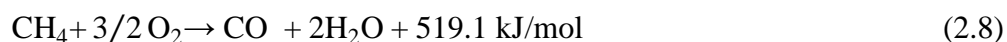
- Partial oxidation of methane to methanol and formaldehyde
- Oxidative coupling of methane
- Conversion to aromatics without an oxidant

A few desired products such as C<sub>2</sub> hydrocarbons, benzene (aromatics), methanol, formaldehyde and carbon in addition to synthesis gas can be formed by direct routes. Among the above approaches, oxidative coupling of methane has received significant attention.

2.2.2.1. Oxidative Coupling of Methane to Higher Hydrocarbons. The oxidative coupling of methane (OCM) involves the reaction of CH<sub>4</sub> and O<sub>2</sub> over a catalyst at high temperatures to form C<sub>2</sub>H<sub>6</sub> as a primary product and C<sub>2</sub>H<sub>4</sub> as a secondary product. Main reactions;



Selective or non-selective reaction occur simultaneously due the gas phase reactions taking place before CH<sub>4</sub> and O<sub>2</sub> contact on the surface of catalyst. The OCM process happens at around 800°C with the limited C<sub>2</sub> products (C<sub>2</sub>H<sub>6</sub> and C<sub>2</sub>H<sub>4</sub>) yield of about 25%; the combustion reaction consumed CH<sub>4</sub> and C<sub>2</sub> products to produce CO<sub>x</sub>.



Ethylene, which is the most important basic chemical for the petrochemical industry, can be obtained from the OCM reaction. Many commercial products such as plastic, resin and fiber can be produced from ethylene; its estimated world demand in 2009 exceeds 140 million tons per year in the petrochemical process with an approximately 3.5% annual

increase (Cameron *et al.*, 2012). It is also used to produce ethanol, which is used to mix in gasoline process. One of the most important uses of ethylene is the production of polyvinyl chloride (PVC) which currently serves over 70% of the construction market, 60% of the wire and cable plastics market and 25% of the coatings. Nowadays, ethanol could be produced commercially from petroleum-based feed stocks by thermal cracking in the presence of steam. In today's economy, a cheaper process of creating ethylene is investigated.

### 2.3. Methane Activation and Reaction Mechanisms

The reaction mechanism of OCM is very complicated. The most important step in this reaction is hemolytic separation of hydrogen atoms from methane by oxygen to produce methyl radicals that combines in the gas phase with another methyl radical or hydrocarbon. The interaction of the gaseous oxygen with an oxide layer forms the surface oxygen ions that can be varied on the surface of the metal oxide catalysts as a form of  $O^-$ ,  $O_2^-$  and  $O^{2-}$ . The form of oxygen ions involved in the reaction influence the activity of the catalyst for OCM reaction; due to abstraction of the hydrogen atom, the C-H bond is broken on the surface (Somayeh *et al.*, 2011).

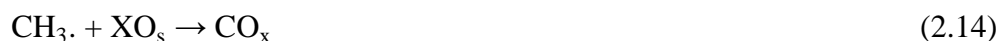


Methyl radical formation, which affects the overall methane conversion, is the slow step of the reactions.

The oxidative coupling of methane reaction first produces ethane by the oxidative dehydrogenation reaction before producing ethylene, which is the desired product of OCM. Methyl radical coupling to  $C_2$  hydrocarbons took place in the gas phase. Then, ethane is oxidized to form ethylene is shown in Figure 2.3.



The undesirable CO and CO<sub>2</sub> formation on the surface limits the formation of ethylene by oxidative coupling reaction; C<sub>2</sub> hydrocarbons with oxygen gas produce CO and CO<sub>2</sub>.



A gas phase reaction between methyl radical and oxygen to produce CH<sub>3</sub>O<sub>2</sub>· radical, which affect the CO and CO<sub>2</sub> formation. The reaction temperature is more favorable for C<sub>2</sub> selectivity because CH<sub>3</sub>O<sub>2</sub>· concentration decreases with increasing temperature; this is one of the reasons why OCM reaction has to be performed at very high temperature.

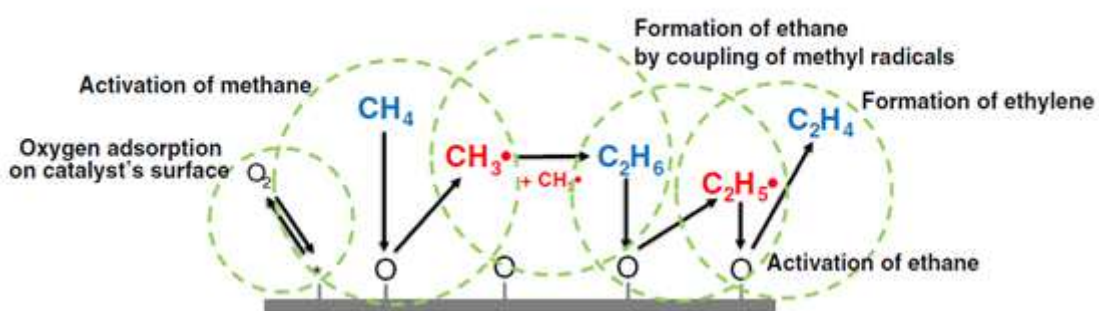


Figure 2.3. Reaction mechanism for the oxidative coupling of methane (Lee *et al.*, 2012).

#### 2.4. Catalysts for Oxidative Coupling of Methane

A catalyst is a substance that accelerates a chemical reaction and effects reaction rate without being affected. The physical (pore size, surface area etc.) and chemical (composition and structure) properties are important factors for a good catalysts. It is generally advantageous to have high surface area to maximize the dispersion of catalytic components. Especially, SiO<sub>2</sub>, TiO<sub>2</sub>, MgO, ZrO, Al<sub>2</sub>O<sub>3</sub> oxide supports show these properties. A catalyst is expected to stay stable during the catalysis process and have thermal strength for OCM reaction.

Oxidative coupling of methane has received a great deal of attention since the fundamental works of Keller and Bhasin (1982). The OCM catalysts need to be active and selective; it should lead to high yield of desired products at low reaction temperatures. In the search for a suitable catalyst, a wide range of supported and unsupported alternatives have been tested by this group between 500°C and 1000°C. It has been found that a wide range of basic oxides, which can be separated into three groups, are effective catalysts: alkali and alkaline earth metal, lanthanide and actinide metal, and transition metal oxide.

#### **2.4.1. The Alkali and Alkali Earth Metal Oxide**

Mostly elements from Group I to II of the Periodic table have been tested for their catalytic activity and stability for OCM. Both alkaline earth (Mg, Ca, Sr, and Ba) and rare earth (La, Ce, Nd, Sm, Gd, Er and Yb) metals play crucial roles in determining the surface properties (basicity/base strength distribution and acidity/acid strength distribution) and activity of the supported catalyst in the process (Choudhary *et al.*, 1999). According to Choudhary and Uphade (2004), the performance of alkali earth metal and promoted rare earth oxide catalysts can be improved by adding an alkaline earth promoter. It is found that the unsupported catalyst such as Nd<sub>2</sub>O<sub>3</sub>, Eu<sub>2</sub>O<sub>3</sub> and La<sub>2</sub>O<sub>3</sub> has a better activity and selectivity with the strong basic sites of La and Nd oxides to develop catalytic activity. It is indicated by Choudhary and Uphade (2004) that the Sr- promoted La<sub>2</sub>O<sub>3</sub> showed the best performance. Both activity and C<sub>2</sub> yield increased by doping the catalyst with Ce and Nd, and addition of 10wt.% ceria (Tiemersma *et al.*, 2012).

Elkins *et al.* (2013) reported that using a typical Al<sub>2</sub>O<sub>3</sub> support prevents the high yield. Changing the properties of Al<sub>2</sub>O<sub>3</sub> is also investigated to obtain a more feasible support. It is observed that, due to the participation from acidic sites which affects the coke formation, it shows lower C<sub>2</sub> selectivity (Elkins *et al.*, 2013).

He *et al.* (2004) studied the preparation of nano-CeO<sub>2</sub>/ZnO catalysts using a novel combination of homogeneous precipitation, and compared it with the conventionally impregnated catalyst for OCM with CO<sub>2</sub> as the oxidant. It is found that there is no correlation between the conversion of methane and the average size of the nanoparticles

but increasing fractal dimensions of nanocatalysts improves the methane conversion. Additionally, they obtained higher methane conversion over the CeO<sub>2</sub>/ZnO nanocatalysts than that over catalysts prepared via conventional impregnation.

Au *et al.* (1998) found that BaO could enhance the activity of Nd<sub>2</sub>O<sub>3</sub>, while BaX<sub>2</sub> could improve the C<sub>2</sub> selectivity in the OCM reaction. When addition of BaX<sub>2</sub> was compared to the undoped Nd<sub>2</sub>O<sub>3</sub>, C<sub>2</sub> selectivity was increased from 33.3 to 50.7% and C<sub>2</sub> yield was increased more than two times at 750°C. Wang *et al.* (1998) investigated the catalytic performance of BaCO<sub>3</sub>/La<sub>2</sub>O<sub>3</sub> catalyst with 0, 2.5, 5, 10, and 15 wt.% BaCO<sub>3</sub> using urea combustion method. The work resulted that the addition of BaCO<sub>3</sub> enhances the performance of La<sub>2</sub>O<sub>3</sub> catalyst. Also, at 550°C, CH<sub>4</sub> conversion and C<sub>2</sub> selectivity were increased from 32.8% to 35.2% and 40.0% to 48.6% respectively while contents of BaCO<sub>3</sub> increases from 0 to 15 wt.% (Au *et al.*, 1998).

The thermal stability of Li, Na and K deposited on MgO, SiO<sub>2</sub>, Al<sub>2</sub>O<sub>3</sub> and Cr<sub>2</sub>O<sub>3</sub> was investigated by Perrichon and Durupty (1988). It was found that, the alkali metals deposited on SiO<sub>2</sub>, Al<sub>2</sub>O<sub>3</sub> and Cr<sub>2</sub>O<sub>3</sub> are more stable than deposited on MgO and a loss of alkali metal was observed at calcination temperatures higher than 500°C. The stability of Li-doped MgO catalysts, the loss of Li, is often discussed in the literature. Arndt *et al.* (1998) shown that the Li-doped MgO is unstable, irrespective of the preparation procedure. Various Li loadings (0, 0.5, 1, 2, 4, and 8 wt.%) were unstable during the test time period of 40 h.; the active Li metal element evaporates from the surface leading to deactivation of the catalyst. Instability of Li limits the lifetime of catalyst and industrial applicability (Tiemersma *et al.*, 2012).

#### **2.4.2. Lanthanide and Actinide Metal Oxide**

In the literature, it is found that adding lanthanides or alkali metals in the OCM catalyst as a promoter improve the selectivity and activity during the kinetic studies. High thermal stability and high productivity of La<sub>2</sub>O<sub>3</sub> promoted by strontium attract some attention and become an interesting study.

The study by Tye *et al.* (2002) was carried out in fixed bed reactor over  $\text{La}_2\text{O}_3/\text{CaO}$  catalyst for isothermal, adiabatic and non-adiabatic operation modes. It was resulted that adiabatic and non-isothermal modes produced low  $\text{C}_2$  yields; higher yield was achieved in non-isothermal conditions.

Choudhary *et al.* (1997) compared the performance of Sr- promoted  $\text{La}_2\text{O}_3$  catalysts with the un-promoted catalyst, which shows lower  $\text{CH}_4$  conversion and  $\text{C}_{2+}$  selectivity. It is indicated in the study that the best results were 30.1%  $\text{CH}_4$  conversion with 65.6%  $\text{C}_2$  selectivity obtained at a temperature  $800^\circ\text{C}$  with the Sr/La ratio of 0.3 and  $\text{CH}_4/\text{O}_2$  ratio 4. The Sr/La ratio influences the performance of the supported catalyst due to its strong basic sites, which are increased with increasing this ratio. The support of the catalyst plays important role to determine the catalytic performance with its surface basicity, larger surface area and lower cost. Another effect was seen at the application in industrial scale reactors: the support causes lower pressure drop across the catalyst bed (Tiemersma *et al.*, 2012).

Oxidative coupling of methane using  $\text{CO}_2$  as an oxidant was studied by Oshima *et al.* (2013) over several La-ZrO<sub>2</sub> catalysts in an electric field. During the conventional reaction catalyst show quite low activity at 1173 K, however with the application of electrical field at 423 K the catalytic activity over the catalyst increased significantly (max. yield 5.4%).

### **2.4.3. Transition Metal Oxides**

Transition metal oxides are quite effective for OCM, especially when they are supported or promoted with alkali metals. Combination of Group V metals of the Periodic Table (vanadium, niobium and tantalum) with Group I metals as a binary and ternary metal oxide catalyst remarkably increase the catalytic performance. Swaan *et al.* (1993) reported on the promoting effect of niobium in a Li/MgO catalyst; under the same operation condition at 873 K, Li/Nb/MgO with 16wt.% niobium shows ten times higher activity than Li/MgO catalyst for OCM. However, when reaction temperature reaches upper than 993 K, catalyst losses its activity because of the melting point of the lithium carbonate phase.

Inert oxides such as  $\text{Al}_2\text{O}_3$ ,  $\text{SiO}_2$ ,  $\text{TiO}_2$  and  $\text{ZrO}_2$  can be used as support to stabilize the active phase. Gong *et al.* (2011) studied the effect of the additives (Li, La, Mn and W) on the catalytic performance of  $\text{TiO}_2$  support; the experiments were carried out at 1043 K with  $\text{CH}_4/\text{O}_2 = 1.4$ . When Li is added as a promoter into  $\text{Mn}/\text{TiO}_2$ ,  $\text{La}/\text{TiO}_2$  and  $\text{La-Mn}/\text{TiO}_2$ , the activity of catalysts decreased; on the other hand, additional of Li metal into  $\text{W}/\text{TiO}_2$ ,  $\text{Mn-W}/\text{TiO}_2$ ,  $\text{La-W}/\text{TiO}_2$  and  $\text{La-Mn-W}/\text{TiO}_2$ , the activity and selectivity increased intensely. They obtained 41.6% methane conversion and 61.7%  $\text{C}_2$  selectivity with 25.6% yield over  $\text{Li-La-Mn-W}/\text{TiO}_2$  catalyst.

Design of a suitable catalyst capable of producing high desired products ( $\text{C}_2$  hydrocarbons) yield at significant level of methane conversion at low temperatures is the key challenge facing the commercialization of OCM. Numerous catalysts have been investigated in OCM reaction; nevertheless the overall  $\text{C}_2$  product yield doesn't exceed 25-30%, which is stated to be insufficient for commercialization of OCM.

In the 1990s, the binary transition metal oxides promoted by alkali metal ions and supported on  $\text{SiO}_2$  or  $\text{TiO}_2$  catalyst has been developed as the new catalysts system for OCM reaction by Fang *et al.* (1993), and published in Chinese. Sofranko *et al.* (1997) studied manganese oxides based catalyst that methane conversion is comparable high with other transition metal oxides in redox cyclic mode of operation. Investigation shows that between the transition metal oxides, only manganese and tin oxides remained stable while the overall  $\text{C}_2$  selectivity was more than 75% at around 1023 K temperature.

Wang *et al.* (1995) studied the oxidative coupling of methane reaction over oxide supported  $\text{Na}_2\text{WO}_4\text{-Mn}$  on  $\text{SiO}_2$  and  $\text{MgO}$  to compare their activities with a pulse reactor. The results indicate that  $\text{CH}_4$  conversion of 20% and  $\text{C}_2$  selectivity of 80% were obtained at  $800^\circ\text{C}$ ; the feed flow included  $\text{CH}_4/\text{O}_2$  ratio of 8/1. This catalyst has a remarkable stability under the high temperature condition.

It was also stated that the best reaction performance only occurs if all 3 metals of this trimetallic system are present for  $\text{Mn}/\text{Na}_2\text{WO}_4/\text{SiO}_2$  catalyst, which is one of the very few suitable alternative for OCM reaction (Li *et al.*, 2003); the presence of tungstate ions enhances the stability of the catalyst, Na-O-Mn species influence the activation of methane. Na-O-Mn and Na-O-W species behaved as an active site on the catalyst (Ji *et al.*,

2002). Sodium is the essential active component; it plays dual roles of which one is to increase the CH<sub>4</sub> conversion and C<sub>2</sub>H<sub>4</sub> selectivity while necessary to reduce the CO formation. Another role of the Na in the catalyst is to prevent the complete oxidation of methane with isolating the Mn ions in Na<sub>2</sub>O, NaO<sub>2</sub> and Na<sub>2</sub>CO<sub>3</sub> surface phase to obtain high selectivity. Moreover, the Na<sup>+</sup> ions lead to increase surface basicity and convert nonselective manganese oxide into a more selective form as reported by Ji *et al.* (2003). In their other work, Ji *et al.* (2002) studied different sodium, tungsten and manganese contents to observe the catalytic performance of the reaction; maximum yield of C<sub>2</sub> was obtained at 1.6wt% Na content. The reaction occurred the best with catalyst content of 0.4-2.3wt.% Na, 0.5-3wt.% Mn and 2.2-8.9wt.% W. Na content influenced the near-surface composition of W and Mn at the catalyst surface; the selectivity to C<sub>2</sub>H<sub>6</sub> and CO increased slightly with the further increase in the Na content of the catalyst while the conversion of CH<sub>4</sub> and selectivity towards C<sub>2</sub>H<sub>4</sub> and CO decreased. When Na loading is above 2.3%, it causes the enrichment of Na near the surface, which implies that the surface concentration of W and Mn decreased greatly. This shows that the migration of W and Mn was carried out with the help of Na<sup>+</sup> ions.

The researches and debates on the active sites on the Mn/Na<sub>2</sub>WO<sub>4</sub>/SiO<sub>2</sub> catalyst are still ongoing. Surface W species including W=O and three W-O-Si bonds enriched with manganese oxide are suggested as the active sites for OCM to provide the exchange between gaseous and lattice oxygen. Kou *et al.* (1997) developed a model and found that oxygen enriched amorphous phases occur from the distributed tetrahedral WO<sub>4</sub> and octahedral MnO<sub>6</sub> groups on the surface of the fresh catalyst. No tungsten species was observed on the used catalyst after a 450 h run. The general formula of tungstate is M<sub>2</sub>WO<sub>4</sub> (M=alkali metals) which consist of tetrahedral ions WO<sub>4</sub><sup>-2</sup>. Firm connection for WO<sub>4</sub> group with the silica surface is not necessary.

Ko *et al.* (1997) also studied the structure of crystalline Mn<sub>2</sub>O<sub>3</sub> and found that tetrahedral transition metal sites (T<sub>d</sub>) were necessary for the activation of methane. Figure 2.4 shows two tentative structural models involving the possible formation of active oxygen species for the surface ensembles.

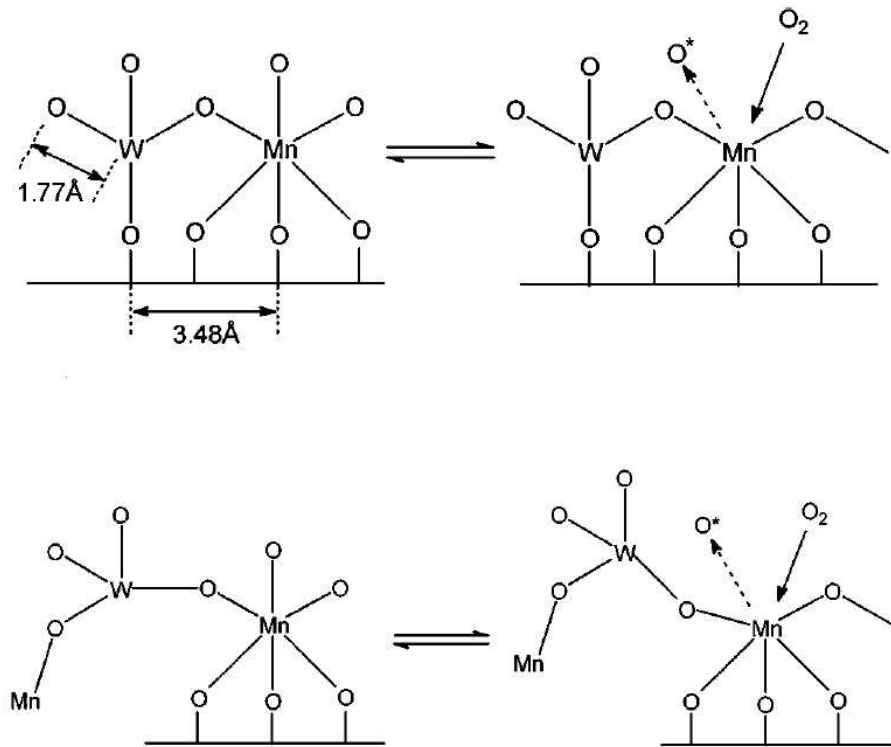
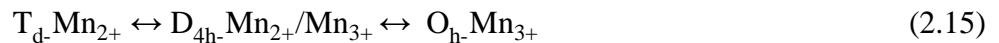


Figure 2.4. Two tentative models involving the possible formation of active oxygen species ( $O^*$ ).

The combination of  $T_d$ - and  $O_h$ - center can transfer electrons and oxygen simultaneously; as a result, the tungsten in a  $T_d$ - center is responsible for the activation of methane while the manganese in an  $O_h$ - center is responsible for the transformation and transportation of oxygen. In the event of  $WO_4$  group disappear from the surface, tetrahedral coordinated  $Mn_{2+}$  species are formed on the surface as a result of the formation of square planer  $Mn_{3+}/Mn_{2+}$ , Therefore,



Kou *et al.* (1997) also suggested that manganese species are good oxygen releaser that accompanied with the tetrahedral transition metal sites ( $T_d$ -) constitute an effective catalytic ensemble for OCM.

Phase transformation from amorphous silica to  $\alpha$ -cristobalite is a significant need for the production of an efficient catalyst. Phase transformation occur the incorporation of W (between  $\text{Na}_2\text{WO}_4$  and  $\text{SiO}_2$ ) with calcination at 750-850°C (Jiang *et al.*, 1993).

Various metal oxides attract interest in the influences of the trimetallic catalyst system to improve the reaction performance. Somayeh *et al.* (2011) investigated the nature of the active sites on the M-Na-Mn/ $\text{SiO}_2$  catalyst (M=W, Cr, Nb and V) using a continuous flow quartz reactor at 750°C and the metal-metal and metal-support interplay effects were studied on the methane conversion and  $\text{C}_{2+}$  yield. The results revealed that addition of W improves the  $\text{C}_{2+}$  selectivity; W is followed by the other metals in the order of  $\text{W} > \text{Cr} > \text{Nb} > \text{V}$  while catalytic conversion did not change significantly. On the other hand, the addition of V, Cr or Nb causes a decrease in the selectivity to  $\text{C}_{2+}$  hydrocarbons. Addition to these studies, Ji *et al.* (2003) modified M-W-Mn/ $\text{SiO}_2$  catalyst with metal oxides; M means a kind of distinct alkali or alkaline earth metals such as Li, Na, K, Ba, Ca, Fe, Co, Ni and Al; the catalyst was prepared by the incipient to wetness impregnation method. They obtained  $\text{CH}_4$  conversion and  $\text{C}_2\text{H}_4$  selectivity of approximately 30% and 40% respectively. The performance of the catalysts was not essentially changed after 5 h time on stream except Li promoted W-Mn/ $\text{SiO}_2$  catalyst. The comparison of the alkali, metal ions and alkaline earth ions showed that the effect of alkali ions was stronger than of the alkaline earth and the other metal ions. It is a critical aim to observe the relationship of the surface morphology and the textural properties and reduction behavior of the catalysts containing different metal oxides. That's why Malekzadeh *et al.* (2007) studied the OCM reaction over metals promoted  $\text{Na}_2\text{WO}_4\text{-MO}_x/\text{SiO}_2$  (M=V, Cr, Mn, Fe, Co and Zn). The results revealed that the  $\text{C}_{2+}$  selectivity enhances with the transition metal composition of the catalyst in the order of  $\text{V} \sim \text{Cr} \ll \text{Fe} \sim \text{Co} \sim \text{Zn} < \text{Mn}$  while methane conversion increases in order of  $\text{V} \sim \text{Cr} \sim \text{Zn} < \text{Fe} \sim \text{Co} < \text{Mn}$ .

Another study was conducted by Chou and co-workers on the influences of  $\text{SnO}_2$  doped W-Mn/ $\text{SiO}_2$  for oxidative coupling of methane to higher hydrocarbons at elevated pressure. A new catalyst was synthesized by the equal-volume impregnation method. The results showed that Mn, Na and W causes migration through the catalyst surface with promotion of adding  $\text{SnO}_2$ ; no direct correlation between the loading content of  $\text{SnO}_2$  and the conversion of methane and selectivity of higher hydrocarbons was found. A

large amount of C<sub>3</sub>-C<sub>4</sub> hydrocarbons were also observed in the final product stream (Chou *et al.*, 2003).

The Mn/Na<sub>2</sub>WO<sub>4</sub>/SiO<sub>2</sub> catalyst has been prepared via various methods such as wet impregnation and physical mixing; however, the incipient to wetness impregnation method has fewer procedure step and easy to control and gives more reproducible results. Li *et al.* (2003) reported that Mn, Na and W are found on the surface when this procedure is implemented; this contributes to the activity of the Mn/Na<sub>2</sub>WO<sub>4</sub>/SiO<sub>2</sub> (Jiang *et al.*, 1993).

Among V, Cr, Mn, Fe, Co and Zn promoted Na<sub>2</sub>WO<sub>4</sub>-MO<sub>x</sub>/SiO<sub>2</sub> catalysts, the catalyst containing manganese oxide shows the best catalytic performance at the OCM reaction conditions. The silica-tungstate and metal oxide-tungstate interaction which occurs during catalyst crystallization also plays a crucial role to determine the catalyst selectivity. The critical parameters for catalysts characterization in the presence of sodium ion (structural promoter) are different metal-metal and metal-supports (chemical promoter) the interactions (Malekzadeh *et al.*, 2007).

As the alternative support material, MgO was also studied instead of SiO<sub>2</sub> with Mn and Na<sub>2</sub>WO<sub>4</sub> elements by Lunsford *et al.* (1998). Lunsford *et al.* investigated the thermal effects during the oxidative coupling of methane over two different catalysts supported on two different support materials: Mn/Na<sub>2</sub>WO<sub>4</sub>/MgO and Mn/Na<sub>2</sub>WO<sub>4</sub>/SiO<sub>2</sub>. Based on their observation in this work, Lunsford *et al.* (1998) proposed that Mn/Na<sub>2</sub>WO<sub>4</sub>/MgO catalyst was deactivated during long times on stream while Mn/Na<sub>2</sub>WO<sub>4</sub>/SiO<sub>2</sub> catalyst shows more stability for longer periods (up to 97 h). The reason of decreasing stability in MgO catalysts was declared as the Mn is lost near the surface region.

## **2.5. Influences of Operating Conditions on the Oxidative Coupling of Methane Reaction**

The reaction network of catalytic oxidative coupling of methane involves many heterogeneous surface and homogenous gas phase reactions that occur in the pores of the catalyst and in the void between the catalyst pellets. During these reactions, absorbed

oxygen species receive H atom from methane that lead to methyl radicals. Primary products, ethane and carbon oxides are obtained as a result of methyl radicals reactions in the gas phase; the methane and C<sub>2</sub>H<sub>4</sub> combustion reactions also produce CO<sub>x</sub>. Only under adjusted reaction conditions (temperature, pressure, residence time, feed composition), the catalytic reactions on the catalyst surface occur before the combustion gas phase reaction took place.

### 2.5.1. The Effect of Feed Gas Composition

Oxygen concentration determines the performance of the OCM reactions leading to fluctuation of the C<sub>2+</sub> selectivity and CO<sub>x</sub> formation. Especially high methane-oxygen ratio is required to minimize thermal effects and to keep methane conversion high (Tiemersma *et al.*, 2012). Karimi *et al.* (2007) showed that lower CH<sub>4</sub>/O<sub>2</sub> ratio lead to a decrease in CH<sub>4</sub> conversion and C<sub>2+</sub> selectivity but an increase in CO<sub>x</sub> selectivity. The optimum CH<sub>4</sub>/O<sub>2</sub> ratio was between 3-4 that increased the rate of C<sub>2</sub>H<sub>6</sub> production and left no extra oxygen available for the combustion reactions which occur at gas phase before methane and oxygen contact on the catalyst surface. When CH<sub>4</sub>/O<sub>2</sub> ratio increases, CO<sub>x</sub> selectivity increases. It is also indicated that the CH<sub>4</sub>/O<sub>2</sub> ratio is related to the thermal effects of the catalyst. The temperature run away was observed at low CH<sub>4</sub>/O<sub>2</sub> ratios (Cameron *et al.*, 1990; Baerns *et al.*, 1994; Pak and Lunsford, 1998).

### 2.5.2. The Effect of Reaction Temperature

Thermal effects during the OCM reactions are highly significant. Selective coupling reactions are more sensitive to temperature changes due to the high activation energy (Tiemersma *et al.*, 2012). Cameron *et al.* (1990) and Baerns *et al.* (1994) pointed out the high magnitude of the temperature profiles (hot spots), which were the results of exothermicity of reaction and are related to the CH<sub>4</sub>/O<sub>2</sub> ratio and catalyst activity. The hot spots of 150°C over a La<sub>2</sub>O<sub>3</sub> catalyst and more than 200°C over a La<sub>2</sub>O<sub>3</sub>/CaO catalyst were reported. Pak and Lunsford (1998) also observed the thermal effects and hot spots during the OCM reaction over Mn/Na<sub>2</sub>WO<sub>4</sub>/SiO<sub>2</sub> and Mn/Na<sub>2</sub>WO<sub>4</sub>/MgO catalysts. They reported

that as a result of the accumulation of reaction heat that occurs in the catalyst bed during the OCM reaction, the temperature has risen as large as 150°C.

### 2.5.3. The Effect of Reactor Pressure

The performance of OCM reactions over Mn/Na<sub>2</sub>WO<sub>4</sub>/SiO<sub>2</sub> catalyst was also investigated over a wide range of total pressure from 100 to 800 kPa even though most of the studies were conducted under atmospheric pressure at which high selectivity and conversion are possible. Ji *et al.* (2002) reported that the elevated pressure is disadvantageous for OCM reaction because of the increasing gas phase reactions. The effect of elevated reactor pressure was also investigated and 16.1% CH<sub>4</sub> conversion with 80.3% C<sub>2+</sub> selectivity at 750°C and 0.6MPa were obtained by Chou *et al.* (2002). Tiemersma *et al.* (2012) reported that the high pressure and high residence time lead to decrease of C<sub>2+</sub> selectivity.

### 2.5.4. The Effect of Residence Time

It was seen in the investigation that all parameters were related to each other and optimizing only one parameter is not enough to succeed the best result for high temperature OCM reactions. To minimize the contribution from any gas phase reaction that occur before CH<sub>4</sub> and O<sub>2</sub> contact on the catalyst surface, an optimum gas hourly space velocity (GHSV) is needed. Karimi *et al.* (2007) varied the residence time from 1300 h<sup>-1</sup> to 2200 h<sup>-1</sup> to observe the changes in selectivity and conversion. When the residence time was too low, combustion reactions took place on the catalyst surface; as a result, C<sub>2+</sub> selectivity decreases. On the other hand, increasing GHSV from 1300 h<sup>-1</sup> to 1920 h<sup>-1</sup> caused an increase in C<sub>2+</sub> selectivity with a decline in methane conversion and CO<sub>x</sub> selectivity. The GHSV more than 1920 h<sup>-1</sup> was also undesirable with the sudden drop in C<sub>2+</sub> selectivity (Tiemersma *et al.*, 2012).

## 2.6. Types of Reactor Used for OCM

Besides the catalyst development, the suitable reactor concepts to make the OCM process technically and economically feasible were also investigated in many publications. A balance between high methane conversion and high selectivity played an essential role to choose the right reactor structure. The counter current bed reactor, solid oxide fuel cell reactor and catalytic dense membrane reactor are the most studied reactor concepts for OCM process while the fluidized bed reactor, porous membrane reactor and fixed bed reactor are also widely investigated (Jašo *et al.*, 2010).

The major problem in OCM process is the formation of hot spots in the catalytic fixed bed reactor which causes undesired side reactions and catalyst deactivation; hence the reactor concept, which doesn't allow effective heat management in exothermic reactions, is not suitable for this purpose. The temperature homogeneity was tried to be achieved with an alternative reactor concept like fluidized bed ensuring isothermal operation condition (Talebizadeh *et al.*, 2009). Comparison between the fixed bed reactor and fluidized bed reactor shows that the fluidized bed reactor has advanced performance with 26% of yield. Unfortunately, it is still under the industrial requirement (Jaso *et al.*, 2010).

The membrane reactors were also studied extensively and show an improved performance in comparison to other reactors. The reaction occurs with oxygen on the catalyst lattice so the contribution of the gas-phase oxygen is mentioned as a deterministic factor to selectivity. This reactor design leads to minimize the gas phase oxygen concentration in the reactor (Talebizadeh *et al.*, 2009). To enhance the C<sub>2</sub> selectivity that is determined by gas phase oxygen, the reactor allows the limited flow of oxygen gas to reaction zone; it also offers the possibility to use air as a cheap oxygen sources. On the other hand, its thermal performance is not as good as that of fluidized bed reactor (Lu *et al.*, 2000).

The significance of the reactor configuration and operating conditions are emphasized in various researches. The Mn/Na<sub>2</sub>WO<sub>4</sub>/SiO<sub>2</sub> catalyst has showed stability for long periods of time under various reaction conditions such as GHSV, temperature and

CH<sub>4</sub>/O<sub>2</sub> ratio (Segei *et al.*, 1998). The paper written by Karimi *et al.* (2007) covers the results obtained under various reaction conditions. They reported that C<sub>2+</sub> selectivity and CH<sub>4</sub> conversion increases with elevating temperature from 780°C to 840°C. When the CH<sub>4</sub>/O<sub>2</sub> ratio is changed from 3 to 5, the methane conversion increased with decreasing C<sub>2</sub>H<sub>4</sub> selectivity; the increment of the CH<sub>4</sub>/O<sub>2</sub> ratio from 5 to 6, on the other hand, reduced C<sub>2</sub>H<sub>6</sub> production due to the lack of oxygen in the feed. CO<sub>x</sub> selectivity is also influenced by residence time, as the increasing GHSV from 1320 h<sup>-1</sup> to 1920 h<sup>-1</sup> decreased methane conversion and CO<sub>x</sub> selectivity. The groups of Lunsford and Lambert reported 80% C<sub>2+</sub> selectivity with 20% and 33% methane conversion respectively (Palermo *et al.*, 1998, Sergei *et al.*, 1998). Ji *et al.* (2002) reported that the best result (37.7% methane conversion and 66.9% C<sub>2+</sub> selectivity) were obtained over 1.9wt.%Mn/5wt.%Na<sub>2</sub>WO<sub>4</sub>/SiO<sub>2</sub> catalyst at 800°C, 48 000 h<sup>-1</sup> methane GHSV and CH<sub>4</sub>:O<sub>2</sub>=3:1 in co-feeding.

### 2.6.1. Microstructured Reactor

Microtechnology is currently growing area; the development of micro structured reactor has been increasingly observed in recent years. Microstructured devices allow us to miniaturize the reaction system that provides less space and energy compared to the conventional chemical reactors. Small dimensions facilitate to develop progressive process units of all sizes with the targeted and adequate microstructured design, thereby enhancing the reactor performance. The size reduction not only leads to integrate multiple devices with new additional function but also make the cost lower.

The microchannel reactor, which has the characteristic dimensions between 10<sup>-3</sup> and 1 mm, usually consist of multiple parallel and identical channels operating in laminar flow regime. These reactors can be also used for the catalytic processes; a thin layer of catalyst with high surface area can be coated on the interior channel walls or packed into the channel as a form of particles (Kolb *et al.*, 2004). When the process requires careful heat management, microchannel reactors seem to be quite suitable for highly endothermic and exothermic reactions such as OCM process, which suffer from the hot spot formation over the packed bed catalysts.

The main advantage of the microreactors is their high surface to volume ratio in the range of 10000-50000 m<sup>2</sup>/m<sup>3</sup> though traditional reactors do not exceed the 100-1000 m<sup>2</sup>/m<sup>3</sup> (Hessel *et al.*, 2004). In addition, high heat transfer coefficient, which is inversely proportional to the ratio of the channel diameter, avoids accumulation of reaction heat within the microstructures so that critical reaction such as exothermic reactions occurs safely at high temperature. Hot spot temperatures due to the exothermicity of the reaction are reduced remarkably so that undesirable side reactions are hindered. Another aspect of microreactor is that the faster heating and cooling of reaction mixtures within the microstructures are possible (Kolb *et al.*, 2004). This superior heat transfer characteristics help to utilize the full potential of catalyst during highly endothermic or exothermic reactions.

Due to the small dimension of reactor system, narrow residence time distribution (RTD) is possible to be obtained in the reactor channel. That brings an advantage for successive process to achieve high selectivity of the desired product (Renken *et al.*, 2005).

Microstructured reactor gives opportunities for new production concept by multiplying the large number of microstructured reactor units without changing the channel geometry. This approach for developing the lab-scale to industrial-scale process system is called numbering-up and it helps to increase the system capacity without reducing the risk of altering the desired critical features of basic units such as tube or vessel diameters (Tonkovich *et al.*, 2005).

The microreactor can be manufactured by different type of fabrication technologies including wet chemical etching, dry etching processes, micro-injection molding, laser ablation, and advanced mechanical processes. Depending upon the industrial area applied and the availability of fabrication techniques, the choice of microreactor material is a key factor. It can be produced from a variety of materials such as metal, polymer, quartz, ceramics or glass.

Another issue in microstructured reactor is the addition of the catalyst into micro-channels. In generally, a solid catalyst is needed to carry out the reactions in microstructured reactor. It is important to obtain a uniform catalyst layer to maintain

catalytic activity with high surface area and an excellent adhesion in coating process. Active phase of the catalyst should be well dispersed for long term stability. Number of methods can be applied to locate the catalyst, including packed the supported catalyst in microchannels and using a chemical vapor deposition (CVD) and physical vapor deposition (PVD), anodic oxidation, sol-gel coating, wash coating, and electro-deposition have been used for catalyst coating of micro-reactors. The catalyst layers deposited on thin film such as metals on the reactor wall by PVD and CVD method leads to low catalyst surface area due to the smooth catalyst films and are restricted to elemental catalysts (Hwang *et. al.*, 2007). Generally, wall coating of catalyst can be applied by two methods dip and spin coating on plates or flat substrate. However these methods are restricted to the formation of submicron layers in porous structures.

The wash-coating technique is the most common way to locate the catalysts within the micro-channels. On the basis of the Ergun equation, packed bed reactors do not perform efficiently because of the pressure drop as the reactor size is scaled down (Fogler, 1992) whereas wall-coated channel geometry can eliminate the pressure drop owing to drag (Şimşek, 2012). The catalyst coated micro-channel has an advantage to reduce the axial and radial temperature gradients in the bed. Thin surface coating of micro-channel minimize the heat transfer limitations herewith providing better heat transfer through channel walls compared to catalyst packing inside the reactor. Therefore, isothermal conditions can be achieved with a lower pressure drop inside the catalyst coated micro-channels.

### **2.6.2. MonoSil Structured Reactors**

The application of microstructured reactors in chemical process industry in the presence of a solid catalyst has gained great attention in recent years. Microstructured systems can be applied with particular success in miniaturization, better control of reaction parameters, safer process operation and easier product recovery. Especially, microreactor system is efficient in experiments of the highly exothermic and fast reaction while reducing the side reactions through the isothermal conditions. Process engineers showed a great development to design small size reactors in the range of few micrometers to a few

tens of millimeters such as multichannel microreactors or macro-/mesoporous monolithic bodies with multimodal porosity (Sachse *et al.*, 2012). It follows that the main feature of these reactors is high surface to volume ratio and very effective reactant mixing within the interconnected nature of their macro-/mesoporous network (Sachse *et al.*, 2012). Therefore, there is a growing interest in mesoporous silica materials such as MCM-41, SBA-15 and silica monoliths.

Mesoporous silicas such as MCM-41 and SBA-16 have highly ordered pore structures. These materials are synthesized with surfactant micelle templates. Surfactants are used as structure directing agents. Surfactants are mixed with silica precursor solution. Pores are shaped with thermal decomposition of the surfactants when the precursor solution is dried and calcined at high temperature. These ordered pores provide using mesoporous silicas as a catalyst support (Kataoka *et al.*, 2009). Additionally, metals and other active compounds can be included into their structure by direct hydrothermal synthesis. Metal precursor is dissolved in a suitable solvent and added dissolved surfactant in deionized water. Silica source is added into this solution (Doğu *et al.*, 2005).

The first macro-/mesoporous monoliths were made by polymers. Kirschning *et al.* (2001) has developed glass/polymer reactors for organic transformations in flow. But the important drawback is pressure drop along the microchannels due to the swelling problems of the polymeric materials. To overcome this, Sachse *et al.* (2009) improved new structured micro reactor that is called as MonoSil or monolithic foam-structured bed that contains silica materials structured macro/mesoporous structure. It is indicated that MonoSils have high chemical and mechanical stability. It is easy to compose organic and inorganic components to form the silica monoliths. Figure 2.5 gives an idea about the form and pore size distribution of the MonoSil.

The common application area of the silica monolithic column is the preparation of high performance columns for liquid chromatography (HPLC). There has been a great interest in the columns that made of porous solids; silica based monoliths looks like a promising alternative. It was reported that the silica monolith can be prepared by polymerization of organic species or polymerization of silicon alkoxides (Ishizuka *et al.*, 2002).

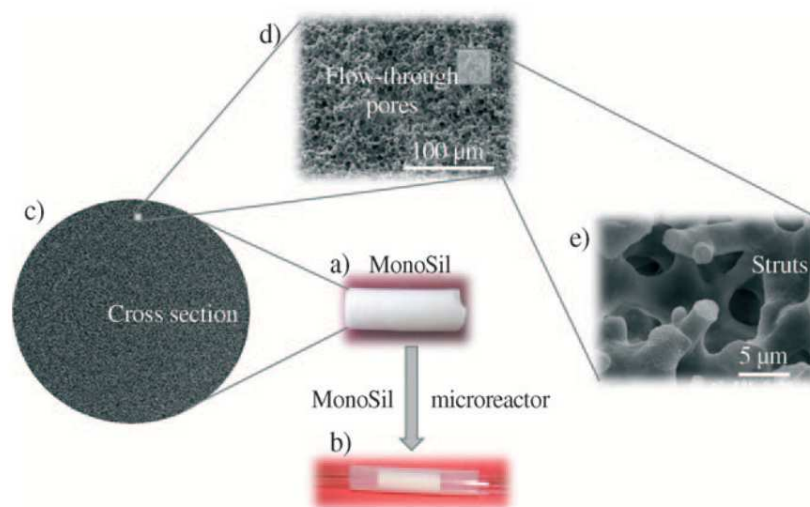


Figure 2.5. The form and pore size distribution of the MonoSil (a) Prepared MonoSil, (b) MonoSil as a microreactor, (c) SEM images, (d) Flow through pores and (e) Struts (Kadib *et al.*, 2009).

Most popular approach to prepare silica based network is sol-gel process, which includes the sequential hydrolysis and polycondensation of alkoxy silicon derivatives (Tetramethylorthosilicate (TMOS) and tetraethylorthosilicate (TEOS)) in the presence of water soluble organic polymers. Tetraethylorthosilicate (TEOS) and polyethylene glycol (PEG) are used as the template materials in preparation of silica monoliths (Siouffi, 2003). PEG is a porogen that plays a role to form of the pores. Concentration of PEG in the solution influences the mechanical properties and pore sizes. Focusing on that point, Nakanishi *et al.* (1998) and Martin *et al.* (2001) investigated that addition of polyethylene glycol decreases the strength of the solid skeleton. The pore size of the porous silica could be modified by changing the concentration of PEG used in the solution. The solution is transformed into gels by aging and drying. The major problem to obtain a silica rod is cracking and shrinkage during the drying. To overcome this challenge, the gel must be dried carefully.

Nowadays, lots of investigations have been focused on improving  $C_2$  selectivity via designing a feasible reactor. The monolithic macro-/mesoporous structure is called attention with their specific properties such as low pressure drop, containable external

porosity and excellent heat transfer capacity. Wang *et al.* (2008) prepared the monolithic foam SiC support containing 5wt.%Na<sub>2</sub>WO<sub>4</sub> and 2wt.%Mn with the dimensions, 20 mm length and 9 mm external diameter. The results showed that the monolithic catalyst represents the same activity at 850°C under the same reaction conditions. During the catalyst bed, hot spot formation is not observed due to its excellent heat transfer feature. Ji and Li (2011) studied on the two-stage catalyst bed reactor with the 2wt.%Mn/5wt.%Na<sub>2</sub>WO<sub>4</sub>/SiO<sub>2</sub> and 5wt.%Na<sub>3</sub>PO<sub>4</sub>/2wt.%Mn/SiO<sub>2</sub> cordierite monolithic catalysts to compare their catalytic performance for OCM. The feed gas firstly passed through the particulate catalyst bed then the monolithic bed. They obtained higher performance (4.8% methane conversion and 2.5% C<sub>2</sub> selectivity) as compared to single particulate catalyst bed.

## 2.7. Methods for Catalyst Preparation

### 2.7.1. Impregnation Method

Impregnation is the conventional method to prepare supported metal catalysts. This method consists of impregnation of a support with the active metal precursors that is dissolved in an aqueous solution. Incipient to wetness impregnation method (IW) provide to the fill pores of the support with the solution. It easy to control and handle the parameters that affect the impregnation method. Impregnation has fewer process steps and gives more reproducible results (Bozorgzadeh *et al.*, 2011).

The common catalyst preparation method for Mn/Na<sub>2</sub>WO<sub>4</sub>/SiO<sub>2</sub> catalyst is incipient to wetness impregnation method. It causes the active component, Mn, Na and W to be well dispersed on the surface. Additionally, due to the very small weight percentage of the active components, below 5wt.% in SiO<sub>2</sub>, those components need to be well impregnated on the catalyst surface for more efficient catalyst (Lee *et al.*, 2012). Li *et al.*, (2006) was compared different catalyst preparation method (impregnation, slurry mixing and wet impregnation) over Mn/Na<sub>2</sub>WO<sub>4</sub>/SiO<sub>2</sub> catalysts, it is resulted that Mn/Na<sub>2</sub>WO<sub>4</sub>/SiO<sub>2</sub> catalysts prepared via incipient wetness impregnation method showed the highest catalytic activity in OCM.

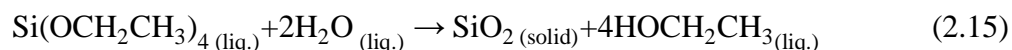
### 2.7.2. Sol-gel Method of Catalyst Preparation

In general, supported metal catalysts can be prepared by various methods. Homogenous mixture of the metal precursors and the support precursors are composed the sol-gel catalysts, which show high dispersion and high thermal resistance to sintering results in the loss of exposed metal surface (Cho *et al.*, 1998).

The sol-gel process roughly represents the route for the formation of a sol followed by that of a gel. A gel means a liquid suspension of solid particles ranging in size 1 nm to 1 micron. Sol-gel is formed from by the hydrolysis and partial condensation of a precursor, for instance, a metal alkoxide and an inorganic salt. A gel is obtained by the condensation of sol particles into three-dimensional network. Polymerization of the particles within the liquid phase constitutes the structures of sol-gel materials which are inherently porous. To remove the trapped liquid in the gel, evaporative drying or supercritical extraction is applied (Ko, 1999). There are four key steps for sol-gel preparation;

- Formation of a gel,
- Aging of a gel,
- Removal of solvent (drying),
- Heat treatment (calcination/sintering)

The precursor, which is a metal salt/alkoxide, is dissolved in an appropriate amount of water or a stable colloidal suspension of preformed sols is used. Metal alkoxides includes aluminates, titanates and zirconates are commercially available in high purity. They have been the most widely used because of their high reactivity. The most widely used non-metal alkoxides are alkoxy silanes, such as tetramethoxysilane (TMOS) and tetraethoxysilane (TEOS). Metal alkoxides are commonly used in the sol-gel process either alone or in combination with non-metal alkoxides such as TEOS or alkoxyborates (Young, 2006). Alkoxide based sol-gel process prevents the formation of undesirable salt and gives an opportunity to control the final product. The chemical equation of the formation of a silica gel from TEOS is given below;



Sol-gel process occurs through two important reactions; hydrolysis and condensation. During hydrolysis, alkoxides reacts with water to form a hydroxide, then condensation occurs to obtain oxide species. The reaction process, hydrolysis and condensation, needs an acid or base catalyst to speed up because of slow reaction of silicon alkoxides with water. Farhad (2000) stated that, for example, the gelation of TEOS in ethanol is reduced from 1000 hours to 92 hours when 0.05 M HCl was added as a catalyst. The pH of the solution affects the reaction rate, thus impacts on the properties of the product. Varying the concentration of catalyst (pH) and type can alter the pore morphology. Under acidic conditions, the hydrolysis happened faster than condensation (Ko, 1999).

Additionally, gel time is another aspect that affects the gel properties. Gel time is defined as the time it takes for a solution to exhibit a rapid rise in viscosity that corresponds to the transition from viscous fluid to an elastic gel (Ko, 1999). Aging represents the time between the formation of a gel and the removal of solvent. When a sol reaches the gel point, it is assumed that the hydrolysis and condensation reactions are over. The solution needs a sufficient time that must be given for the strengthening of the silica network for gelation. The parameters that influence the aging process are temperature, time and pH of the pore liquid. Sol must be immersed or washed with another liquid, exposing gel to a different humidity, heated to change these parameters (Ko, 1999).

Drying is the final process to obtain the linked silica network without the liquid which is evaporated from the gel. A capillary pressure associated with the liquid-vapor interface within a pore becomes an issue while the liquid is removed from the pore. Drying process can be performed carefully to minimize the differential pressure or capillary pressure to maintain the integrity of a gel network (Ko, 1999).

Further heat treatment is required in order to burn off any residual organics or to oxidize the sample after removing the liquid in the pore. Generally, heating is applied in the presence of a reactive gas (Ko, 1999). As a result of sintering and decrease in the

surface area can be observed if the sample exposed to a high temperature over a prolonged time.

It was indicated by Lambert and Gonzalez (1998) that this method has an advantage such as superior homogeneity and purity and better microstructural control of the support. On the other hand, many catalysts need further thermal treatment and careful drying process to prevent cracking to obtain desired physical properties. In spite of the advantages of the sol-gel method, it has not found wide application in commercial catalyst production except in case of some carriers such as alumina, silica alumina and hydrotalcites from alkoxides and hydrothermal synthesis of zeolites (Özdemir, 2003).

Li *et al.* (2006) studied the OCM reaction over Mn-Na<sub>2</sub>WO<sub>4</sub>/SiO<sub>2</sub> catalysts prepared by various methods such incipient wetness impregnation method, mixture slurry method and sol-gel method. Comparable experiments showed that under the same reaction condition, catalysts prepared by these methods showed the same C<sub>2</sub> selectivity; additionally, catalyst prepared by sol-gel method performed lower C<sub>2</sub>H<sub>4</sub> and CO selectivity. On the other hand, increasing temperature range from 780°C to 860°C, CH<sub>4</sub> and O<sub>2</sub> conversion increased while no leaping increase was observed for the other two catalyst preparation method.

### **2.7.3. Monolithic Catalyst Preparation**

The term “monolith” comes from Greek language, combination of mono, means “single” and lithos means “stone”. In heterogeneous catalysis, it is carried out a catalyst support that has to be chemically inert against reactants and products. A monolithic catalyst support can be coated with different organic or inorganic phases depending on reaction. Monoliths are the large uniform block of a single building material such as ceramic (mainly cordierite) or metal (stainless steel or metal alloy) (Tomašić and Jović, 2006). Despite of better mechanical durability of metallic monoliths at high temperature, they show less thermal stability compared to the ceramic monoliths. (Pérez-Cadenas *et al.*, 2005). The cordierite monoliths that are used in the experiment are shown in Figure 2.6.

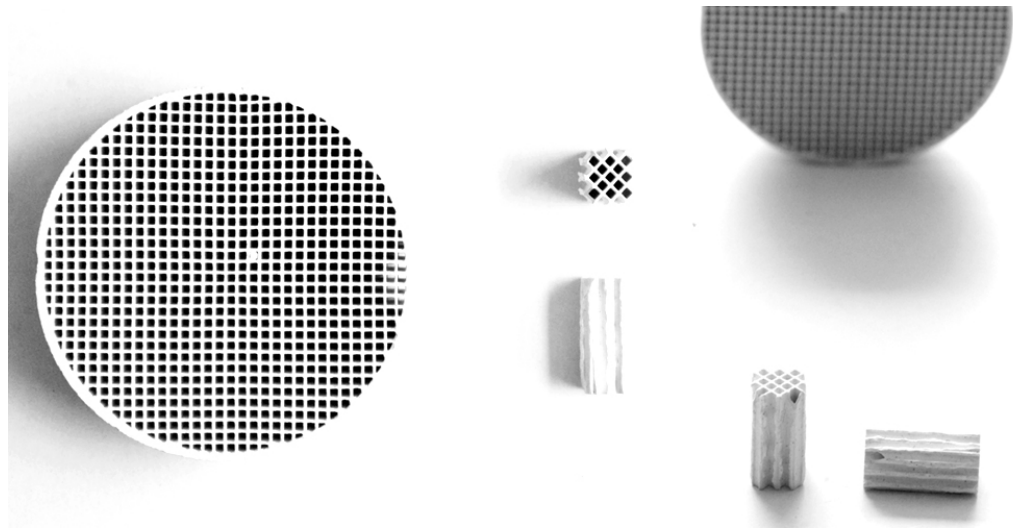


Figure 2.6. The monolithic structure used in the experiments.

General application of monolithic catalysts is the automobile exhaust treatment, natural gas engine and hydrogen generation for the fuel cell. Monolithic catalyst provides high specific area and good interphase mass transfer; on the other hand it has a laminar flow regime that leads to a high residence time distribution that is undesired for high conversion levels (Özdemir, 2009).

The bare cordierite monoliths have a low surface area (generally  $0.7 \text{ m}^2/\text{g}$ ) (Özdemir, 2009) that is not sufficient for the catalytic application. The active phase is needed to be deposited on the walls or inside the walls of inert monolith to increase the surface area. If the monolith structure is available in the required support material, the catalytically active phase can be directly deposited on the monolith. However, if the monolith is not available in the required support material then this support material should be coated on the monolithic substrate first. The process is called as wash-coating (Figure 2.7). Coating of the monolith structure can be done by various methods; with colloidal solution of the appropriate support (the support is in the form of suspended particles, with sol-gel method (the support is in the liquid phase) and with adequate suspensions and other procedures (Tomašić and Jović, 2006). The well-known way to apply well-dispersed coating layer is colloidal coating method. The colloidal solution of silica or alumina is commercially available. The general route to follow the wash-coat methods is done firstly wetting or

filling the channels with the coating solution and then clearing the channels by forcing the air through them. Lastly, drying and calcination of the monolithic support structure.

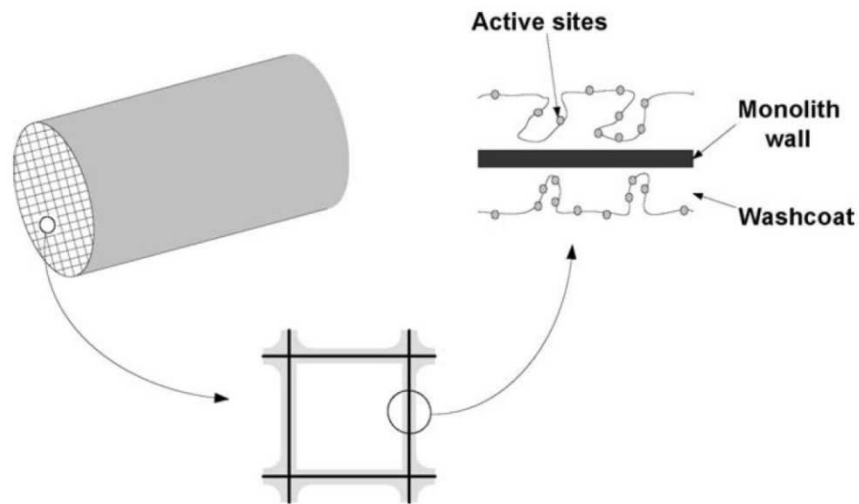


Figure 2.7. Schematic diagram of a monolith structure (Tomašić and Jović, 2006).

The second step to obtain the active monolithic catalyst gets through impregnation the active elements. The key point is the well dispersion and homogeneous distribution of active phase on the catalyst layer. The active elements can be deposited over monolithic structure during wash-coating step or using with the other methods such as precipitation, impregnation, co-impregnation and ion exchange. The drying process is done into microwave or at room temperature.

### 3. EXPERIMENTAL WORK

#### 3.1. Materials

##### 3.1.1. Chemicals

All the chemicals used for catalyst preparation are presented in Table 3.1 and Table 3.2 shows the specifications of the gases used in the study.

Table 3.1. Chemicals used in catalyst preparation (all specifications: research grade).

Chemicals	Formula	Source	Molecular Weight (g/mol)
Silica Gel	SiO <sub>2</sub> (60 - 100 mesh) (200 - 245 mesh)	Sigma Aldrich	60.08
Manganese II nitrate tetrahydrate	Mn(NO <sub>3</sub> ) <sub>2</sub> *4H <sub>2</sub> O	Merck	251.01
Sodium tungstate dihydrate	Na <sub>2</sub> WO <sub>4</sub> *2H <sub>2</sub> O	Sigma Aldrich	329.85
Colloidal silica (40 wt.% Suspension in H <sub>2</sub> O)	SiO <sub>2</sub>	Sigma Aldrich	60.08
Polyethylene Glycol 20,000	HO(C <sub>2</sub> H <sub>4</sub> O) <sub>n</sub> H	Merck	20000

Table 3.1. Chemicals used in catalyst preparation (all specifications: research grade)  
(cont.).

<b>Chemicals</b>	<b>Formula</b>	<b>Source</b>	<b>Molecular Weight (g/mol)</b>
Tetraethylorthosilicate (TEOS)	$C_8H_{20}O_4Si$	Merck	208.33
Nitric Acid 65%	$HNO_3$	Sigma Aldrich	63.01
Acetic Acid	$CH_3COOH$	Merck	60.05
Ammoniac Solution 25%	$NH_3$	Aksın	17
N-Cetyl-N,N,N-trimethylammonium Bromide (CTMABr)	$C_{16}H_{33}N(CH_3)_3Br$	Merck	364.45

### 3.1.2. Gases

Table 3.2. Specifications and applications of the gases used in the study.

<b>Gas</b>	<b>Specification</b>	<b>Application</b>
Helium	99.998%	Inert, GC Carrier Gas
Methane	99.995%	Reactant, GC calibration
Oxygen	99.999%	Reactant, GC calibration
Carbon Dioxide	99.999%	Product, GC calibration
Carbon Monoxide	99.990%	Product, GC calibration
Ethylene	5%	Product, GC calibration
Ethane	5%	Product, GC calibration
Mixture	5% Methane 2% Ethane 2% Ethylene	Product, GC calibration

### 3.2. Experimental Systems

The experimental systems used may be divided in two groups:

- (i) **Catalyst Preparation Systems:** The catalysts were prepared in various methods; incipient to-wetness impregnation of active metals, preparation of catalysts with sol-gel method and direct hydrothermal synthesis method (MCM-41). Then, the particulate catalysts were used directly or coated on the cordierite monolithic support and FeCrAl alloy plate. Additionally, the prepared slurry and gels were applied to load the active metals on the supports.
- (ii) **Catalytic Reaction System:** The catalytic activity of the catalysts was tested in a micro-reactor flow system includes gas flow control, temperature controlled reaction chamber, feed and product sampling sections. This system is used for determining the catalytic activity and selectivity.

### 3.2.1. Catalyst Preparation and Pretreatment

The following methods were employed to prepare catalysts that are used in this thesis.

3.2.1.1. Particulate Catalyst Preparation with Impregnation Method. Mn/Na<sub>2</sub>WO<sub>4</sub>/SiO<sub>2</sub> particulate catalyst containing 2wt.%Mn and 5wt.%Na<sub>2</sub>WO<sub>4</sub> supported on SiO<sub>2</sub> were prepared by sequential or co-impregnation to incipient wetness of silica gel using the system in Figure 3.1 with an aqueous solution of Mn(NO<sub>3</sub>)<sub>2</sub>tetrahydrate and aqueous solutions of Na<sub>2</sub>WO<sub>4</sub>dihydrate.

Commercial silica gel support was first sieved into suitable mesh size and then calcined in a muffle furnace at 500°C for 4 h to avoid support from turning into gel form. Silica gel was washed 3 times using boiled distilled water to remove possible impurities such as Fe and Na and then dried in furnace at 115°C overnight and calcined again in air at 500°C for 4 h before used as a support as reported in article written by Mo *et al.* (2009). After some experiments, this method was given up and support material was used directly. 60-100 mesh (0.250-0.149 mm) and 200-400 mesh (0.074-0.0037 mm) mesh size of pure silica gel was used as a support material.

Figure 3.1 used for preparing particulate catalysts by incipient to wetness impregnation technique consists of a Retsch UR1 ultrasonic mixer, a vacuum pump, a Büchner flask and a MasterFlex computerized-drive peristaltic pump for preparing particulate catalysts by sequential incipient to wetness impregnation technique.

For the preparation of catalysts by incipient to wetness sequential-impregnation method, a definite amount of silica gel support was put in a vacuum flask and was kept under vacuum in the first step. The support material in the vacuum flask was mixed under vacuum with an ultrasonic mixer for 30 minutes before impregnation.

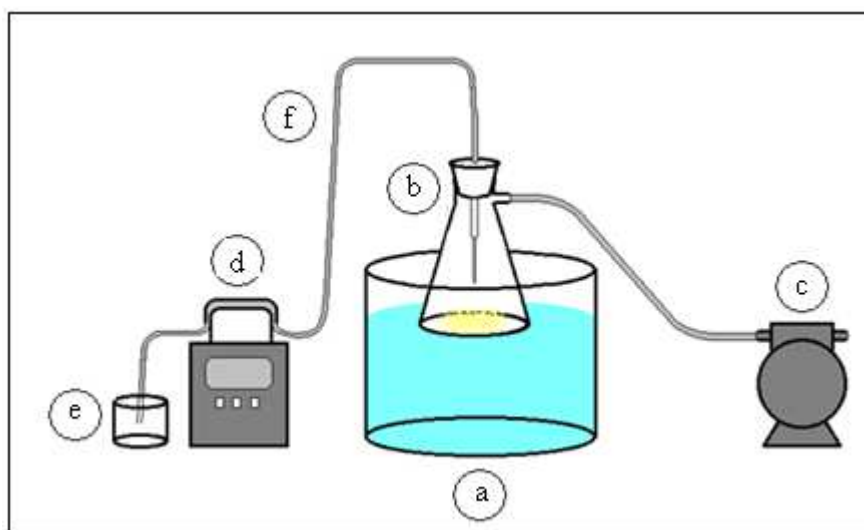


Figure 3.1. Schematic diagram of the impregnation system

(a) Ultrasonic mixer, (b) Büchner flask, (c) Vacuum pump, (d) Peristaltic pump, (e) Reactant storage tank and (f) Silicone tubing (Yoğurtçu, 2012).

The appropriate amount of  $\text{Mn}(\text{NO}_3)_2$  tetrahydrate aqueous solution was dissolved in deionized water on the basis of 1 g silica gel/1.1 ml solution at  $85^\circ\text{C}$ . Then, prepared solution fed to the vacuum flasks at a flow rate of  $0.5 \text{ ml}\cdot\text{min}^{-1}$  by a silicone tubing using with a Masterflex computerized-drive peristaltic pump. After all solution was fed, it was ultrasonically mixed under vacuum during impregnation process to obtain uniform distribution of the aqueous solution. The resulting slurry was dried at  $130^\circ\text{C}$  for 5h. After cooling to  $25^\circ\text{C}$  appropriate amount of  $\text{Na}_2(\text{WO}_4)\cdot 2\text{H}_2\text{O}$  with deionized water based on 1 g silica gel/1.2 ml solution is prepared. Then, the slurry used as a new support material and put in a flask to mix with an ultrasonic mixer for 30 minutes before impregnation. The calculated amount of aqueous solution of  $\text{Na}_2\text{WO}_4$  dihydrate was fed to the vacuum flask at the same condition of first impregnation. When all solution was fed, the slurry ultrasonically mixed during impregnation. The final slurry was dried at  $130^\circ\text{C}$  overnight then calcined at  $800^\circ\text{C}$  for 8 h to obtain  $\text{Mn}/\text{Na}_2\text{WO}_4/\text{SiO}_2$  particulate catalyst.

3.2.1.2. Particulate Catalyst Preparation with Sol-gel Method. The sol gel catalyst was prepared by the composition of the metal precursors and the support precursors from a homogeneous solution (Cho *et al.*, 1997).

Sol gel catalysts were prepared using the system shown in Figure 3.2. The sol-gel preparation system consists of a heater which is also used as a electronic agitator, pH meter and thermometer. The beaker was isolated to prevent heat removal. Temperature and pH of the solution was controlled with pH meter and thermometer during the process.

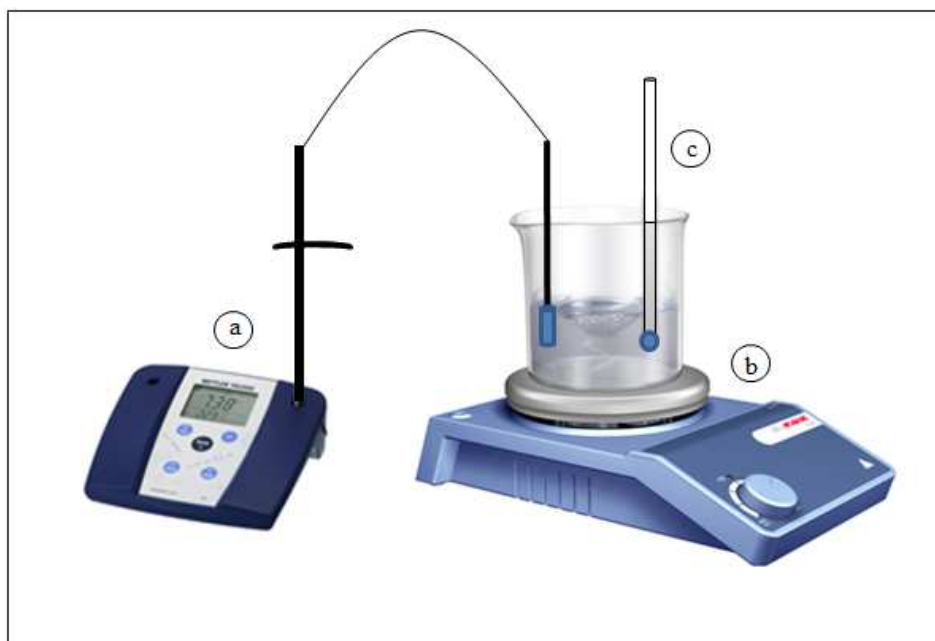


Figure 3.2. Schematic diagram of the sol-gel system  
(a) pH meter, (b) Heater and (c) Thermometer.

The calculated amount of  $\text{Mn}(\text{NO}_3)_2$  tetrahydrate was mixed with 24 ml of distilled water and 1 ml HCl (36.5%). Solution was stirred continuously and heated at  $80^\circ\text{C}$ . Then, 48 ml ethanol and 37.18 ml tetraethoxysilane were added drop by drop into the solution and stirred totally 1 h until getting form of a gel. Mn coated silica gels were dried at  $70^\circ\text{C}$  for 12 h and calcined at  $450^\circ\text{C}$  for 4 h. The appropriate amount of  $\text{Na}_2\text{WO}_4$  was impregnated on the Mn-silica gels by using incipient to wetness impregnation procedure as mentioned in Section 3.2.1.1.

3.2.1.3. Preparation and Pretreatment of Wall Coated Catalysts. The synthesis of particulate catalyst with 200-400 mesh size (0.074-0.0037 mm) silica gel support was prepared by the same procedure summarized in 3.2.1.1 for the preparation of the catalyst layer used in the wall-coated geometry. The metallic plate coated was made of FeCrAl alloy (Good fellow) and has dimensions of 2 mm x 5 mm x 25 mm (height x weight x depth). Before wall-coating process, all plates were cleaned then plates were heat treated in air at 900°C during 2 hours with a heating rate 10°C/min to obtain rough surface composition of Al<sub>2</sub>O<sub>3</sub> which was reported to improve the adhesion of the coating (Aartun *et al.*, 2004).

Wall coating process consists of mixing the appropriate amount of catalyst powder as slurry and then coating the surface with this slurry. The mixed slurry was prepared in two different ways; without any  $\gamma$ -Al<sub>2</sub>O<sub>3</sub> support and 20wt.%  $\gamma$ -Al<sub>2</sub>O<sub>3</sub> support. The first slurry was prepared using 5wt.%Mn/2wt.%Na<sub>2</sub>WO<sub>4</sub>/SiO<sub>2</sub> catalyst, which was prepared by incipient to wetness impregnation technique and deionized water. The second slurry is prepared by the combination of 20wt.%  $\gamma$ -Al<sub>2</sub>O<sub>3</sub> support and 80wt.% 5wt.%Mn/2wt.%Na<sub>2</sub>WO<sub>4</sub>/SiO<sub>2</sub> catalyst using the same procedure. The catalyst slurry is carefully coated as a thin layer on one side of the metallic plates by using a thin blade. Finally, the powder coated plates are dried at 120°C 24 h, then calcined at 500°C during 2 hours.

3.2.1.4. Preparation and Pretreatment of Monolithic Support with Wash-Coating. The commercial ceramic (2MgO.2Al<sub>2</sub>O<sub>3</sub>.5SiO<sub>2</sub>) cordierite monolithic support was first wash coated with silica to obtain high surface area on the surface of the monolith structure coated by colloidal solution. Then the active elements, Mn and Na<sub>2</sub>WO<sub>4</sub> were impregnated on the silica coated monoliths. The Mn and Na<sub>2</sub>WO<sub>4</sub> percentage were held the same as the particulate catalyst: 5wt.%Mn and 2wt.%Na<sub>2</sub>WO<sub>4</sub>.

The commercial monolith was cut into the dimensions of 17 mm length and 8 mm diameter so that it can be easily placed into the 10 mm ID quartz tube reactor. The shaped monoliths were washed with acetone in order to remove the possible impurities and open the pores from residue from the cutting procedure and dried in the oven.

One group of the cordierite monoliths was wash-coated with silica via colloidal solution as shown in Figure 3.3. The bare monoliths were weighed first and then it was immersed vertically into the 40wt.% colloidal silica solution using an ultrasonic mixer to be interpenetrated the silica homogenously all around the monoliths during 40 min. In every 10 min., the excess solution inside the channels was removed by flushing thoroughly with pressurized air, then the monoliths were dried in microwave oven operated at 180 W for 40 min. and weighed again.

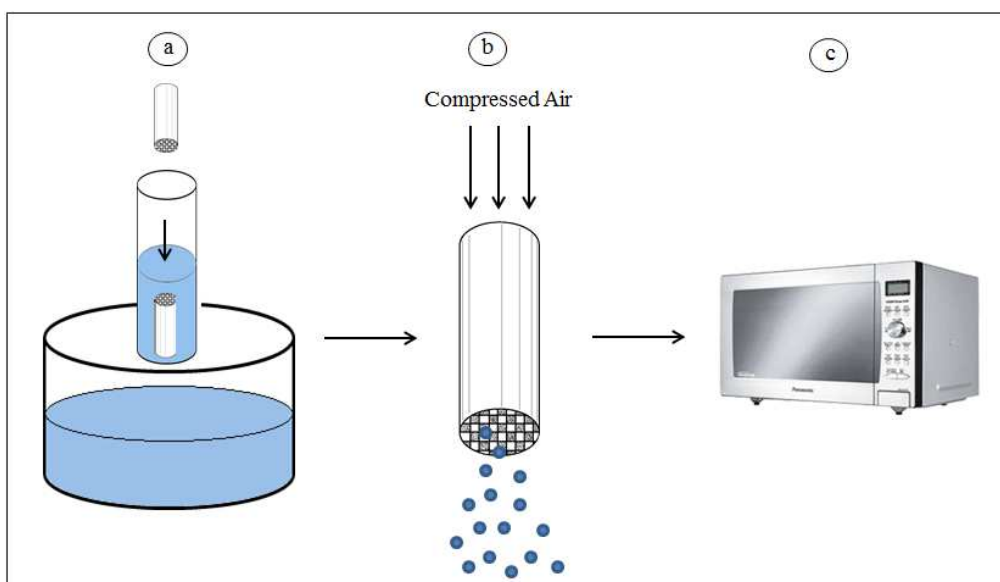


Figure 3.3. The monolith coating system (a) Dipping Procedure in Ultrasonic mixer, (b) Compressed Air Flow and (c) Microwave Oven.

Sol-gel method was applied to coat the second group of cordierite monoliths. Sol-gel preparation was described in Section 3.2.1.2. After pretreatment process, monoliths were weighed and then dipped vertically into the sol-gel solution for two minutes. The excess of the gel in the channels was removed by flushing with an air flow. The monolith cylinders were dried at 70°C for 12 h and calcined at 450°C for 4 h.

The loading of Mn and Na<sub>2</sub>WO<sub>4</sub> promoter to the silica coated monolith support was achieved by immersing appropriate amount of promoter added solution. The monoliths were weighed before and after coating with a colloidal silica solution. The difference between two weights was taken as the SiO<sub>2</sub>coated, and the amount of Mn and Na<sub>2</sub>WO<sub>4</sub>

promoters was calculated on 2wt.% and 5wt.% respectively based on the weight of coated silica. Firstly, appropriate amount of  $\text{Mn}(\text{NO}_3)_2 \cdot 4\text{H}_2\text{O}$  was dissolved at  $85^\circ\text{C}$  in deionized water and silica coated monoliths were immersed it during 40 min. while ultrasonically mixing. Then it was dried at  $130^\circ\text{C}$  for 5 h. After cooling, monoliths were immersed in appreciate amount of  $\text{Na}_2\text{WO}_4 \cdot 2\text{H}_2\text{O}$  aqueous solution with ultrasonically mixing during 40 min. After loading two promoters, the monoliths are dried at  $130^\circ\text{C}$  for 5 h before being calcined in air at  $800^\circ\text{C}$  for 8 h.

3.2.1.5. Monolithic Catalyst Preparation with Sol-gel Method. Synthesis of macro-/mesoporous silica monoliths is a new alternative route to obtain enviable size of catalyst. The silica monoliths were prepared based on the sol-gel method prepared by Sache *et al.* (2012). 46.3 ml distilled water and 3.2 ml  $\text{HNO}_3$  were first mixed at  $0^\circ\text{C}$ . After mixing 15 min., 4 or 4.79 gr. (both amount were tested) polyethylene glycol 20.000 (PEG) was added and continuously stirred for 1 h in ice bath. Then, 40.4 ml tetraethoxysilane was added and stirred for another 1 h. After that, the resulting solution was filled into plastic syringes and glass tube. The solution was kept at  $40^\circ\text{C}$  for 3 days in order to complete gelation. The monoliths removed from their molds, washed in water and treated in an ammonia solution (0.01 M) at  $40^\circ\text{C}$  for 20 h. After neutralization, monoliths were dried at  $40^\circ\text{C}$  for 24 h in an oven and finally calcined at  $550^\circ\text{C}$  for 8 h. The prepared silica monoliths were then used as the support material and loaded Mn and  $\text{Na}_2\text{WO}_4$  elements using by incipient to wetness impregnation method as mentioned in Section 3.2.1.1.

One part of the gel was prepared with 4.9 gr. PEG and it was used as particulate monolithic catalyst. It was not possible to obtain a whole structure with this amount of PEG adding in the solution. The monolithic whole structure could be obtained with adding 4 gr. PEG in the solution as shown in the Figure 3.4.; these monoliths were used as whole structured catalysts in the experiments.

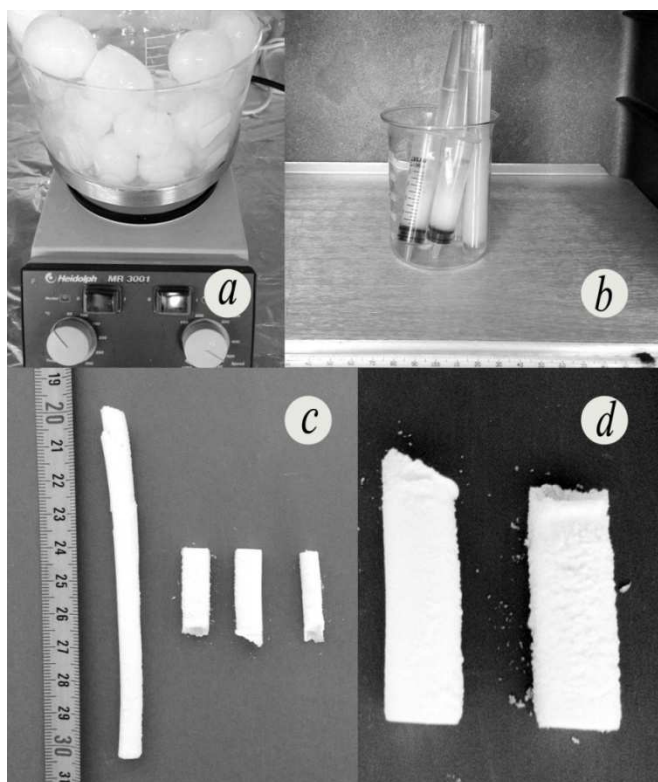


Figure 3.4. Preparation of Monolithic catalyst (Monosil) with sol-gel method (a) Preparation step, (b) Aging in the oven, (c) and (d) Monolithic catalyst (Monosil).

**3.2.1.6. Preparation of Mn-MCM-41 Catalyst Support.** Mn incorporated MCM-41 support catalyst was prepared by direct hydrothermal synthesis method. Amount of manganese was based on the silica weight in silica source. The catalyst was prepared by the same weight percentage of the particulate catalyst (2wt.%Mn and 5wt.%Na<sub>2</sub>WO<sub>4</sub>) metal precursors. Appropriate amount of Na<sub>2</sub>WO<sub>4</sub> dihydrate was added to the support material by incipient to wetness impregnation method as mentioned in Section 3.2.1.1.

Preparation procedure for MCM-41 used was adapted from Doğu *et al.* (2005). Cetyltrimethylammonium bromide (CTMABr) was used as surfactant. 13.2 gr. surfactant (CTMABr) was dissolved in 75 ml deionized water, while the solution was heated up to about 30°C for complete dissolution of CTMABr. As a silicate source, 15.7 gr. sodium silicate was added drop by drop in the solution with continuous mixing. Appropriate amount of metal precursor was added at this step. Important parameter was the pH of the solution; it must be 11. Then, 0.01M acetic acid is added after sodium silicate into the

solution until the pH reaches 11 (the solution turns into a gel form). The gel was put in the oven at 120°C during 96 h. The formed mixture was filtered and washed with deionized water until the pH of the filtrate was about 7. The prepared washed product was dried at 40°C 24 h. To remove the organic compounds in the pores, the product was calcined. The furnace temperature was increased from room temperature to 550°C at a heating rate of 1°C/min and continued for 6 h at 550°C. Schematic diagram of synthesis of MCM-41 is shown in Figure 3.5. To obtain desired catalyst, calculated amount of Na<sub>2</sub>WO<sub>4</sub> dehydrate was impregnated on the calcined product and the following steps were applied in Section 3.2.1.1.

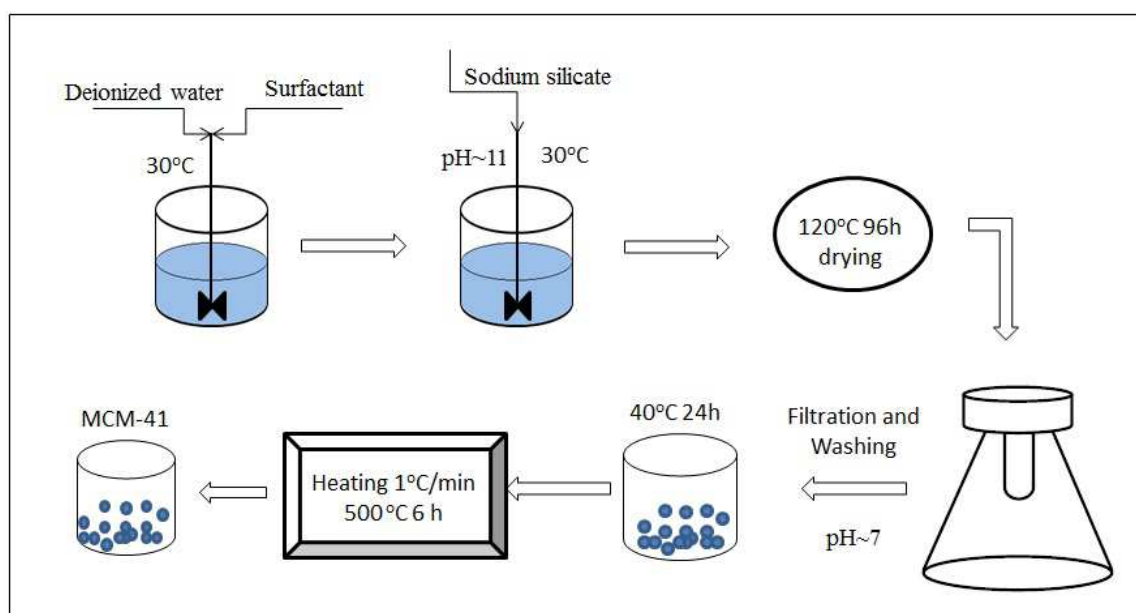


Figure 3.5. Synthesis process of MCM-41.

### 3.2.2. Catalytic Reaction Tests for OCM Reaction

The catalytic micro reaction system shown in Figure 3.6 was designed and constructed in the Catalysis and Reaction Engineering Laboratory of Chemical Engineering Department, Boğaziçi University and involved three distinct sections for feed adjustment, catalytic reaction and product analysis.

1/4", 1/8" and 1/16" OD stainless steel and copper tubing, valves with stainless steel and brass fittings for feeding gaseous species were used in the system. The flow rates of research grade high purity gases (oxygen, helium) from pressurized cylinders passed through the system were regulated with Omega Model 5878 digital mass flow controllers of which set values were adjusted by the main control unit. Additionally, methane gas was delivered to the system with Brooks 5850E mass flow controllers.

Reactant gases (oxygen and methane) without diluents, after being mixed, were sent into the reaction section which consists of 10 and 20 mm ID quartz, 10 mm ID quartz becomes narrow to 2 mm ID quartz fixed bed down flow reactor (Figure 3.7), for conventional packed bed experiments. Quartz tubes were connected with two custom design fittings to the 1/4" stainless steel main line. The total length of the reactor was 80 cm, which was longer than the furnace tube so that the fittings of the reactor can be kept out of the furnace to facilitate manipulation during catalyst charging or recharging. Catalytic zone contains the 100 mm long constant temperature zone of a 30 mm ID x 600 mm tube furnace with a K-type thermocouple was attached to the outside wall of the reactor to monitor reaction zone temperature and control the furnace. The quartz reactor was placed into the furnace controlled to  $\pm 0.1$  K by a Shimaden FP-21 programmable temperature controller. The reactant mixture entering and product leaving the reactor were passed through two ON-OFF valves to either the GC sampling that was calibrated before to analyze the gas mixture or to outside passing through the soap bubble meter for measuring the flow rate of the effluent at the ambient temperature.

One part of the study included wall coated and packed micro-channel reactor. The tests were done at 700, 750 and 800°C at atmospheric pressure with different CH<sub>4</sub>/O<sub>2</sub> ratio in feed stream to obtain the best results.

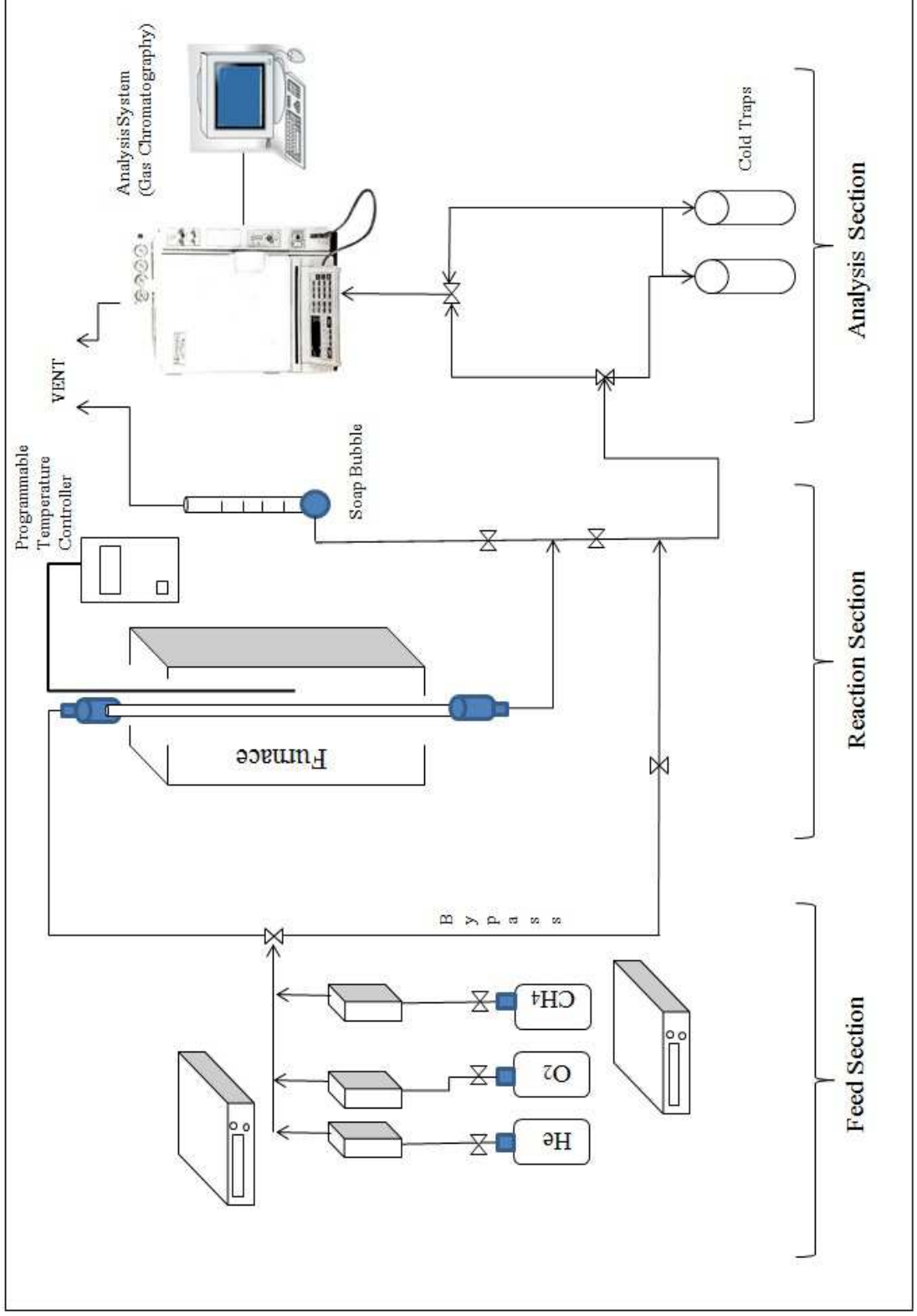


Figure 3.6. The micro reactor flow system and product analysis system.

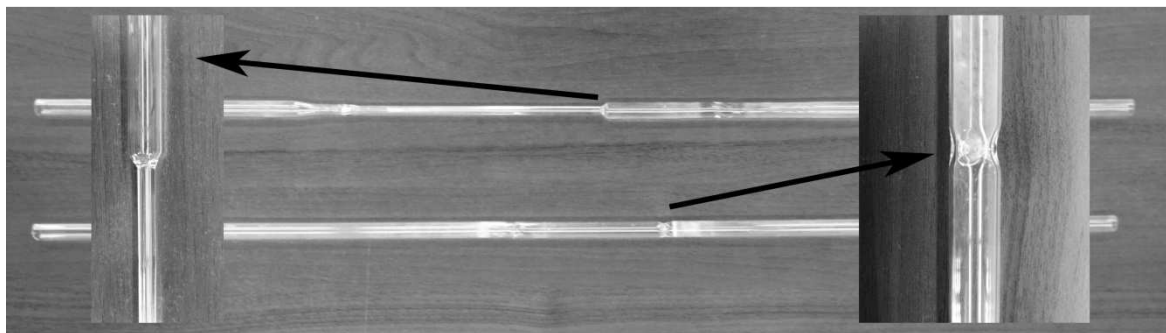


Figure 3.7. 10 mm and 10 to 2 mm narrower ID quartz fixed-bed down flow reactor.

The microchannels in the reactor were formed by using a cylindrical engineered metal housing made of 310-grade stainless steel with external dimensions of 18.6 mm x 30 mm (outer diameter x length). The interior of the housing is shaped with the wire electro discharge machining technique that leads to insert the coated plate in the channel. The channel has 0.75 mm x 4 mm x 25 mm (height x width x depth) (Figure 3.8). The coated and packed tests were done with FeCrAl alloy plate in this housing. The particulate catalyst was filled into the channels between the uncoated plates. A ceramic wool plug (Shimadzu) is placed into the last 5 mm gap between the end of the plate and the housing to prevent the movement of the plate. The same procedure was followed for inserting the coated plate.

Particulate catalysts were inserted into the 10 mm ID quartz down flow reactor. Quartz tube reactor design was modified, and down of the reactor was made narrow to remove the gasses quickly after the catalyst layer. First, the catalyst filled into reactor directly, then lower and above part of the catalyst layer in the quartz tube was filled with quartz chips, silica particles or quartz sand. To prevent the mixing of the particulate catalysts and quartz chips, ceramic wool is used before and after the catalysts part (Figure 3.9). Total feed stream was 52 ml/min and 100 ml/min within the temperature range between 600-800°C. The catalyst was oxidized with O<sub>2</sub> during heating the furnace until the desired temperature. The heating was started after 400°C with 10 ml/min flow of oxygen.

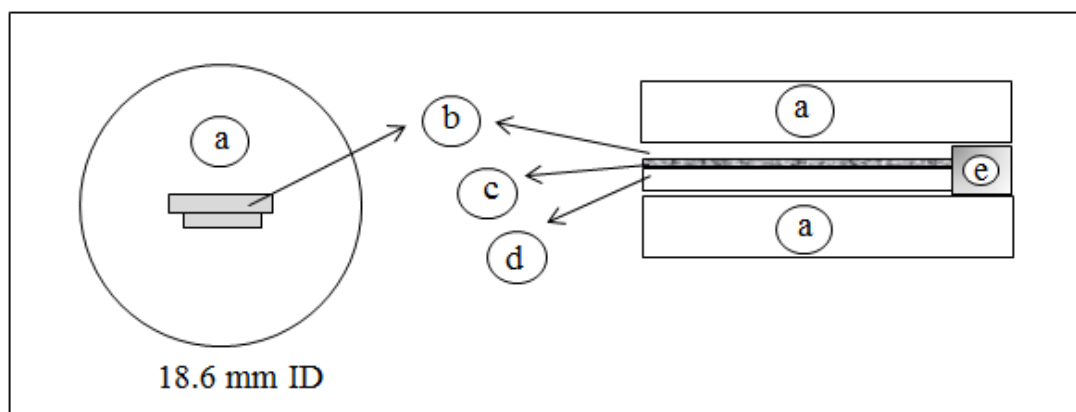


Figure 3.8. Top (at the left) and cross-sectional (at the right) view of the coated microchannel configuration; (a) Engineered metal housing, (b) Open microchannels, (c) Coated catalyst layer, (d) FeCrAl alloy plate and (e) Ceramic wool plug (Şimşek, 2012).

Coated cordierite monoliths were filled in the 10 mm ID quartz tube reactor. Three coated cordierite monoliths were used as a catalyst (Figure 3.9). One bare monolith catalyst support weight is around 0.810 gr. (Its catalyst weight was around 0.22 gr.); hence three monoliths had catalyst approximately equal to the amount of particulate catalyst used. Bare cordierite monolith supports were coated with two ways; one was coated via colloidal silica solution (it was successfully coated 27wt.%), the other way was dipping the monoliths into the sol-gel solution (5wt.% coating is succeed).

The furnace that heats the reactor was heated up with 10°C/min. After each 200°C, the temperature was held steady for 5 min. then continued to heat up.



Figure 3.9. Quartz tube reactor filled with quartz chips (a) Whole reactor, (b) Particulate catalyst, (c) Particulate catalyst (crushed monolithic particulate) and (d) Cordierite monoliths.

### 3.2.3. Product Analysis System for OCM Reaction

During the experiments, the product mixture contained unreacted methane and oxygen and product gases involving hydrogen, carbon dioxide, carbon monoxide, water, ethylene and ethane. A Shimadzu GC-14A gas chromatograph equipped with a Thermal Conductivity Detector (TCD) was used to analyse feed and dry product streams. Analysis conditions were given in Table 3.3. The column was conditioned first at 250°C during 5 h to ensure removal of possible impurities on packing materials.

Table 3.3. Reactant and product gas analysis conditions.

GC	A Shimadzu GC – 14A
Detector type	TCD
Column temperature, °C	200
Injector temperature, °C	170
Detector temperature, °C	230
Detector Current, mA	100
Carrier gas	Helium
Carrier gas flow rate, ml/min	25
Column Packing Material	Carboxen 1000, 80-60 mesh
Column Tubing Material	Copper
Column Length & ID	210 x 3 mm
Sample loop	1 mL

Before proceeding with the experiments, the gas chromatograph was calibrated by injecting known amounts of the gases to be analyzed under the conditions given in Table 3.3. Using this procedure, volume versus peak area curves were obtained for each gas and the corresponding calibration factors were determined by linear regression.

## 4. RESULTS AND DISCUSSIONS

### 4.1. Preliminary Work

Mn/Na<sub>2</sub>WO<sub>4</sub>/SiO<sub>2</sub> is one of most extensively studied catalyst in the literature with high selectivity and yield; however, the conventional reactors that are generally used in these studies have the problem of poor heat removal. To test the applicability of micro-structured reactors, which are known for better heat management, the initial experiments were performed using the most commonly catalyst properties and reaction conditions reported in the literature in two micro-structured reactors.

#### 4.1.1. Experimental Results on the Coated Catalyst Layer on the FeCrAl Alloy Plate

The first experiments were done by coating a 2 mm x 5 mm x 25 mm (height x width x depth) FeCrAl alloy plate (contains 70wt.%Fe, 25wt.%Cr and 5wt.%Al) with Mn/Na<sub>2</sub>WO<sub>4</sub>/SiO<sub>2</sub> catalyst placed in the metal house with 0.5 mm distance between the plate and the grooves. The plates were exposed to heat treatment to obtain rough surface structure so that they can hold the catalyst particles better. The catalyst coating process was lead to give a total remaining coating mass of 7.2-7.7 mg coated catalyst layer on the plate. Unfortunately, the results were shown that adhesion of the catalyst to the surface was quite poor; it was very easy to remove the catalyst layer on the FeCrAl alloy plate with a small physical exertion.

The reaction tests were performed with a 20 mm ID quartz reactor the under the CH<sub>4</sub>/O<sub>2</sub> ratio of 7.4, the temperatures of 750°C and 800°C and flow rate of 100 ml/min (23% He was used as diluents) considering the reaction conditions proposed by Lunsford *et al.* (1998) in their communication. Unfortunately 60wt.% of the catalyst was lost during the reaction. As a solution of this problem, 20wt.% α-Al<sub>2</sub>O<sub>3</sub> was mixed with catalyst powder to obtain more adhesive catalyst layer. However the adhesion stability of oxide layer to the FeCrAl alloy substrate was not improved significantly although the conversion and selectivity was not decreased sharply. As indicated by Figure 4.1, 750°C was better for

selectivity while 800°C resulted higher conversion although the yield (conversion x selectivity) is much lower than that is reported (about 20-25%) in the literature.

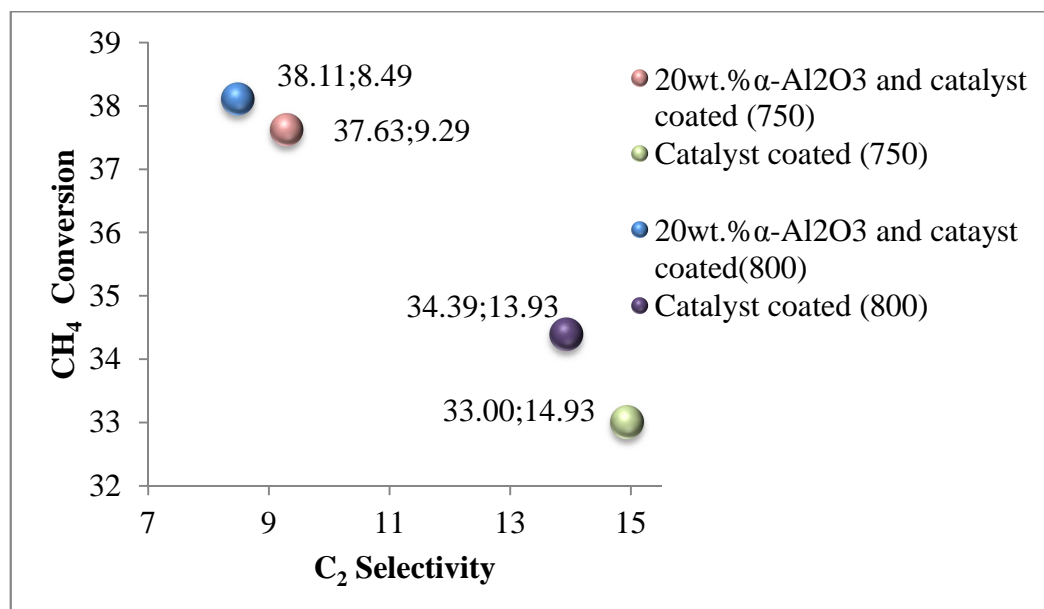


Figure 4.1. Results of the experiments of comparison of the coated catalyst layer with the 20wt.%  $\alpha$ -Al<sub>2</sub>O<sub>3</sub> included catalyst coated layer.

Zhang *et al.* (2012) discussed the difference between the metallic (such as FeCrAl alloy) and conventional non-metallic supports. The weakness of adhesion of the oxide layer to the FeCrAl alloy substrate was attributed to the differences between the properties of the metallic support and oxide layer; this constitutes a significant limitation for using a metal as a catalyst support. Coating the silica support material on the FeCrAlloy plate was a real challenge; it could not be strongly bonded with Al<sub>2</sub>O<sub>3</sub> surface to adhere stably on the metal alloy support.

#### 4.1.2. Experimental Results on the Catalyst Coated on the Cordierite Monolithic Support

Catalyst coating on the monolithic structure is an alternative way to have the active metals on the surface of regular channel structure. The advantages of monolithic supports are stated as low diffusion resistance, excellent mass and heat transfer (Ji and Li, 2011). It

has been widely used in catalytic combustion and partial oxidation of methane reactions. Jing-jing *et al.* (2009) studied the preparation of M-W-Mn/SiO<sub>2</sub>/cordierite monolithic catalysts and their performances for oxidative coupling of methane while Liu *et al.* (2008) synthesized Na<sub>2</sub>WO<sub>4</sub>-Mn/SiC monolithic foam catalyst for the same purpose. These researches showed a promise for using monolithic catalyst over OCM reactions.

The monolithic supports, cut with the sizes of 8 mm diameter and 17 mm length were coated in two ways; sol-gel coating and coating by a silica colloidal solution. In both methods, 2wt.%Mn and 5wt.%Na<sub>2</sub>WO<sub>4</sub> were added by incipient to wetness impregnation method on the silica coated structure. The monolithic channels that were coated 5wt.% silica by sol-gel coating method and the same amount of active metal coated over 12wt.% silica by colloidal silica solution coating were compared with 0.2 gr. particulate catalyst in Fig. 4.2. Experiments were done under the same reactor that were used in micro-structured metallic channels (temperature 750°C and CH<sub>4</sub>/O<sub>2</sub> ratio is 3 with 10 mm ID quartz reactor).

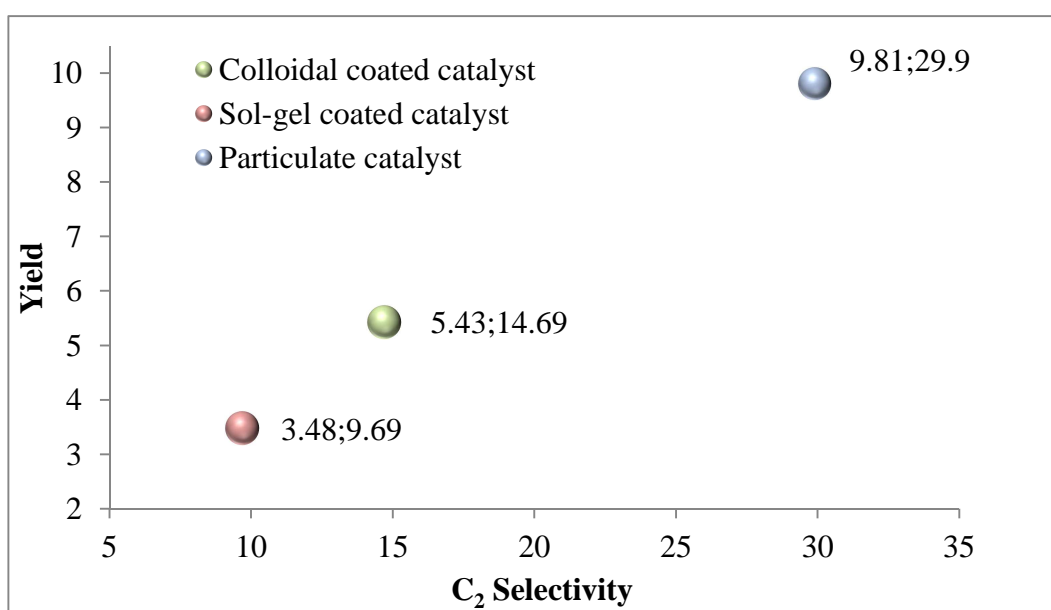


Figure 4.2. Effect of using cordierite monolithic support with different coating methods.

Although the results over the wash coated monoliths were much better than those over the FeCrAl alloy plate, they were not as successful as the particulate catalyst. When the monolithic support was coated by colloidal silica support to improve the catalyst

surface area, it was observed that more the coating was succeed. The results also showed that catalyst coated by the colloidal solution showed better performance than the catalyst coated by sol-gel method.

## 4.2. Design of the Reactor

### 4.2.1. Reactor Tube Diameter

The initial microstructure reactor experiments were done using 20 mm ID quartz tube reactor to place metal housing or monolithic support. However a new quartz tube reactor was designed and decreased the initial diameter 10 mm to 2 mm as shown in the Figure 3.7. Although CH<sub>4</sub> conversion was the same as the value obtained constants 10 mm ID reactor, the C<sub>2</sub> selectivity was increased from 25.78% to 37.55% when the experiment were done with particulate catalyst. Similar results were observed through the years by various investigators. For example Lunsford (1998) used fused-quartz tubing reactor with the internal diameter decreasing from 7 mm to 2 mm. The catalyst was placed the bottom of the 7 mm ID part so that the residence time after the catalyst would be decreased to avoid decomposition of products in gas phase reactions. The following researches were also done using reactors with decreasing diameter after the catalyst bed with significant improvement in performance (Talebizadeh *et al.*, 2008; Lee *et al.*, 2012; Talebizadeh *et al.*, 2009).

### 4.2.2. Reactor Filling Material

The investigations for the enhancing the C<sub>2</sub> selectivity by Lunsford (1998) and Ji *et al.* (2003) pointed out that the space above and below the catalyst bed need to be filled with some porous material to decrease the temperature gradient in the catalyst bed and minimize the contribution of gas phase reactions that decompose products. Hence various filling material were also tested in this work as discussed below.

The first experiments were performed using 45-60 mesh size particulate catalyst (prepared by impregnation method) by filling the empty volume above and below the catalyst bed with 6 cm length 45-60 mesh size  $\alpha$ -Al<sub>2</sub>O<sub>3</sub> particles resulting some

improvement in  $C_2$  selectivity (Figure 4.3); then all empty space was filled with same material (meaning that nearly 40 cm of the quartz reactor- more than the length of furnace- was filled) with some minor change in the result. The full filling of the reactor means the filling above and below of the catalyst bed, it was more than the length of the furnace. This improvement suggested testing various types of materials to improve  $C_2$  selectivity. Then, the reactor was filled with pure crushed  $SiO_2$ , quartz sand and 18-140 mesh size quartz chips. Pure crushed  $SiO_2$  and quartz sand was not suitable material for filling apparently due to their small particle sizes; they stuck and blocked the gas flow in the reactor. Then the bigger (uncrushed-3/16 inches spheres)  $\alpha-Al_2O_3$  particles was tested and it reduces the coke formation around the catalyst bed and provided small increase in the  $C_2$  selectivity when compared with the smaller mesh size. Hence larger sizes quartz chips (obtained by crushing quartz glass) was used as a filling material to reduce the reactor volume. As presented in Figure 4.3, the large size quartz chips showed the best catalytic activity and doubled the  $C_2$  selectivity at around approximately the same  $CH_4$  conversion level. Experiments were done at the temperature  $750^\circ C$  and  $CH_4/O_2$  ratio is 3 with 10 mm ID quartz reactor.

Figure 4.3 shows the improvement of the catalytic performance due to the changes of the filling material. The yield was minimum in the absence of filling material; also the pure crushed  $SiO_2$  showed the same performance as the non-filling. Using  $\alpha-Al_2O_3$  particles as a filling material was a good solution; a better yield was obtained with the increasing particle size. However the real significant improvement in performed was obtained with using quartz chips. Lunsford (1998) explained that the quartz chips helps to preheat the reagents and decrease the free volume; hence the materials should provide excellent heat transfer without affecting the gas flow.

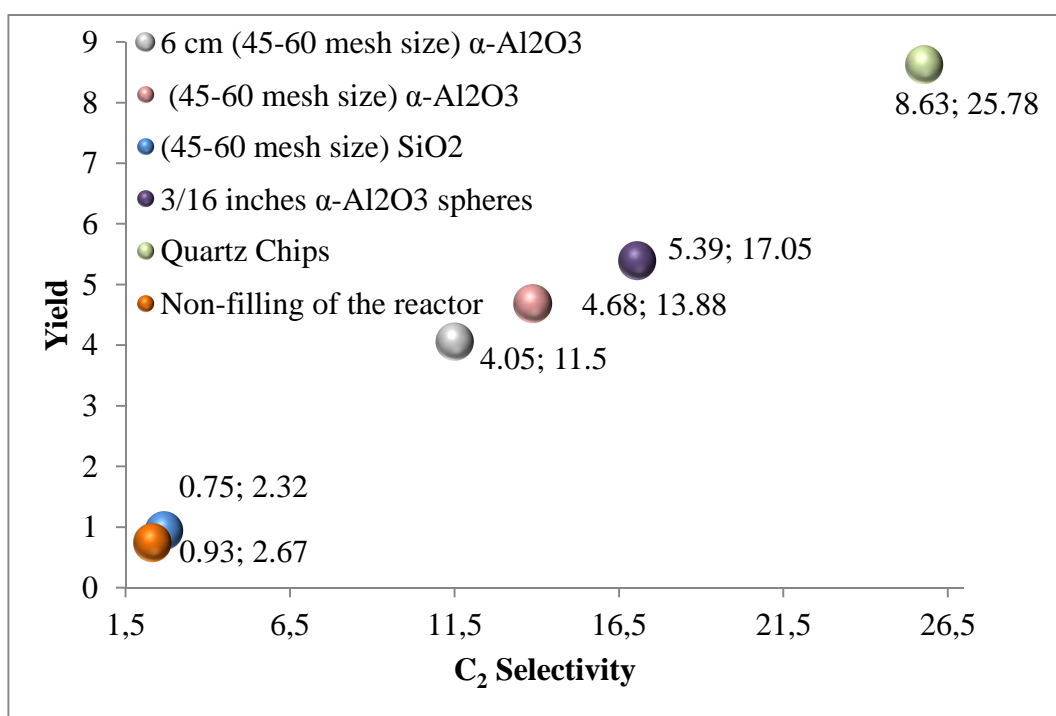


Figure 4.3. Effect of using different kinds of filling material.

### 4.3. Effects of Catalyst Preparation and Operational Conditions

Preliminary works showed that even a small change on the reaction system may have significant impacts. Although the reactor structure and filling material have provided some improvement, they were not sufficient; the influences of catalyst preparation and operating conditions on the OCM that cannot be ignored. For instance, Talebizadeh *et al.* (2009) emphasized the importance of the space time, temperature and CH<sub>4</sub>/O<sub>2</sub> ratio in any reliable kinetic mode. Another study on the operating conditions were conducted by Karimi *et al.* (2007) to show that the performance of the OCM reaction is feasible and economical under only certain reaction conditions.

#### 4.3.1. Effects of Operational Conditions

The experiments were carried out at atmospheric pressure over Mn/Na<sub>2</sub>WO<sub>4</sub>/SiO<sub>2</sub> 45-60 mesh size particulate catalysts prepared via incipient to wetness impregnation method, 100ml/min feed stream without any diluents. The reaction temperature tests were

changed in the range of 600°C-800°C whereas the CH<sub>4</sub>/O<sub>2</sub> ratios of 3, 7 and 10 were studied. 0.2 gr. Mn/Na<sub>2</sub>WO<sub>4</sub>/SiO<sub>2</sub> particulate catalysts were loaded in the catalyst bed and the rest volume of the reactor was placed with quartz chips. The reactor was heated up with 10ml/min flow of O<sub>2</sub> after 400°C until the desired temperature to oxidize the catalyst (Palermo *et al.*, 1998; Talebizadeh *et al.*, 2008).

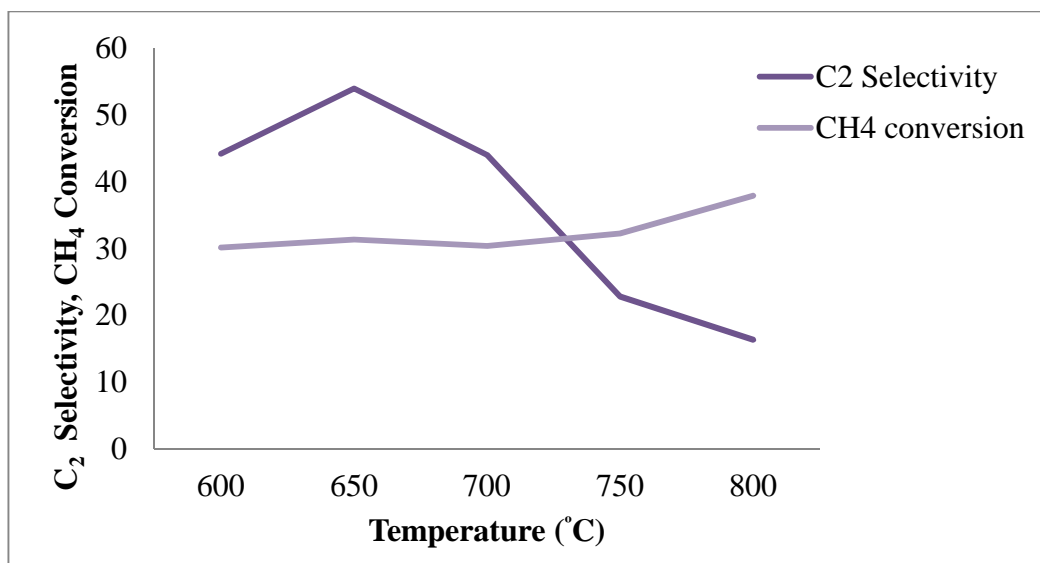


Figure 4.4. Effect of reaction temperature on the CH<sub>4</sub> conversion and C<sub>2</sub> selectivity, CH<sub>4</sub>/O<sub>2</sub> ratio is 7.

Figure 4.4 shows the results of the effect of reaction temperature; the C<sub>2</sub> selectivity decreased significantly with increasing in the reaction temperature from 600 to 800°C while the CH<sub>4</sub> conversion was slightly enhanced. Methane conversion was increased from 30.18% to 37.95% with increasing temperature from 600 to 800°C; this increase, however, was mostly observed at 750°C. Talebizadeh *et al.* (2009) attributed the decline of selectivity with the deep oxidation of ethane and ethylene to CO<sub>2</sub> and CO. Wang *et al.* (2005) observed that CO was mainly produced by the deep oxidation of C<sub>2</sub> hydrocarbon in OCM reaction.

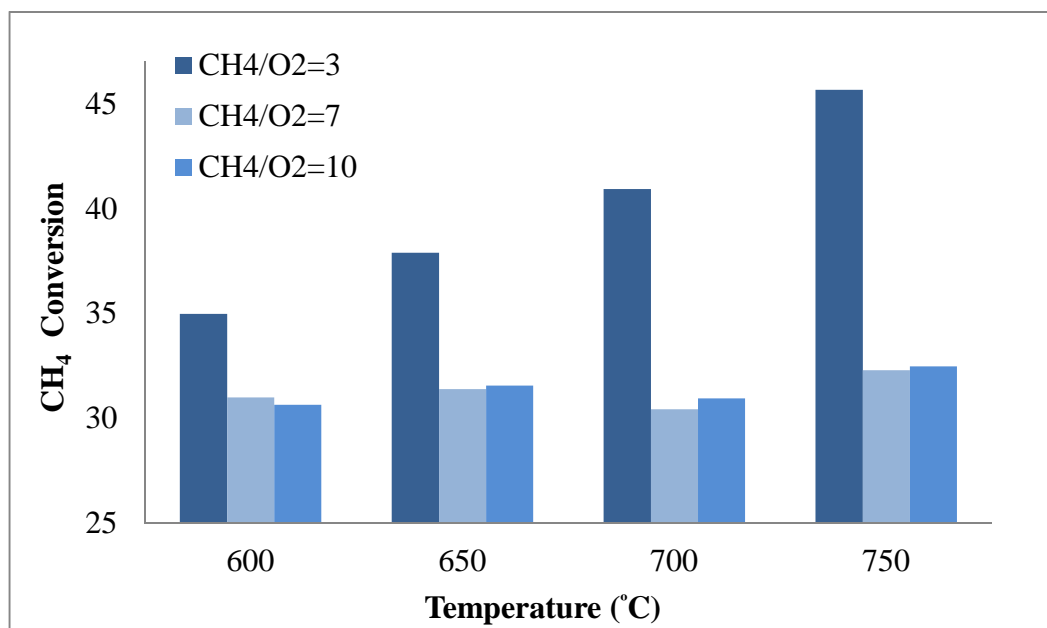


Figure 4.5. Effect of CH<sub>4</sub>/O<sub>2</sub> ratio on the CH<sub>4</sub> conversion at different temperature

Figure 4.5 compares the effects of CH<sub>4</sub>/O<sub>2</sub> ratios at various temperatures. When the CH<sub>4</sub>/O<sub>2</sub> ratio was 3, sharp increment of the methane conversion was observed and (highest 45.7%) while no significant change was observed at higher CH<sub>4</sub>/O<sub>2</sub> ratios. Unfortunately, neither high temperatures nor low CH<sub>4</sub>/O<sub>2</sub> ratios favor the C<sub>2</sub> selectivity. The characteristic behavior in OCM reaction over various catalysts was that the C<sub>2</sub> selectivity was higher at higher CH<sub>4</sub>/O<sub>2</sub> ratios (Wang *et al.*, 2005; Tebibzadeh *et al.*, 2009). During the experiments, the highest selectivity was obtained at highest CH<sub>4</sub>/O<sub>2</sub> ratio as shown in Figure 4.6. The C<sub>2</sub> selectivity was maximized (55.8%) at the temperature of 650°C and CH<sub>4</sub>/O<sub>2</sub> ratio of 10, and decreased with further increase of temperature.

The results in Figure 4.6 shows that the high yield can be obtained at 650°C with CH<sub>4</sub>/O<sub>2</sub> ratio were 7 and 10. The conversion was not maximized at this point but the selectivity was more important (considering that the conversion is not also too low at this condition). Lunsford *et al.* (1998) reported the best operating conditions as the CH<sub>4</sub>/O<sub>2</sub> ratio of 7.4 and the temperature of the thermocouple on the outside of the reactor was 800°C. They observed a temperature gradient cross the catalyst bed and indicated that decreasing CH<sub>4</sub>/O<sub>2</sub> ratio causes higher temperature gradients. For example, when the CH<sub>4</sub>/O<sub>2</sub> ratio was 5, the temperature difference between the center of catalyst bed and the

reactor wall was as high as 150°C while the CH<sub>4</sub>/O<sub>2</sub> ratio of 10 caused only 50°C temperature increment. This explains why the nominal temperature of 650°C (measured outside of reactor) is more favorable since it corresponds to a sufficiently higher temperature since the higher measured temperatures means that the catalyst bed temperature is too high for OCM reaction.

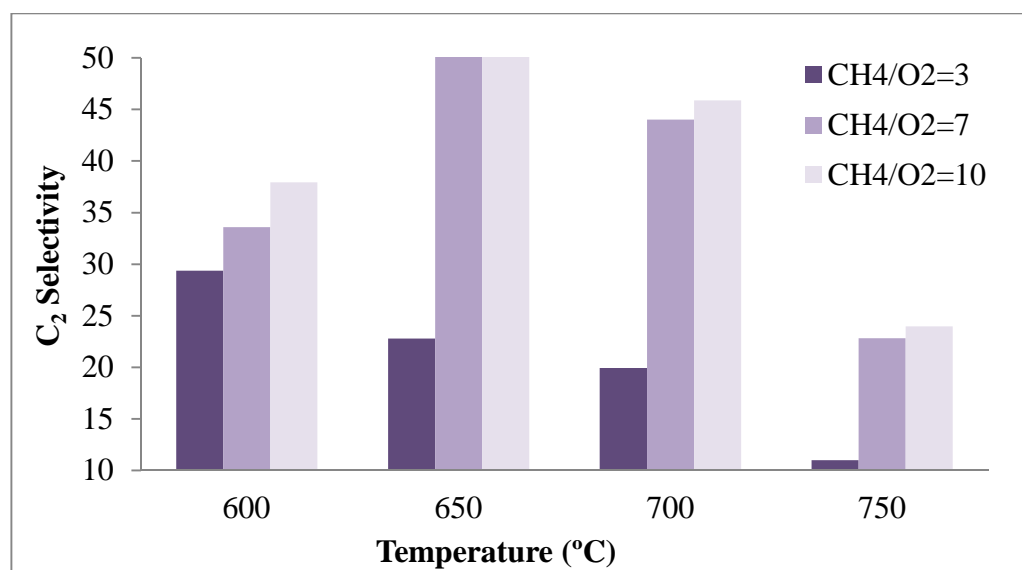


Figure 4.6. Effect of CH<sub>4</sub>/O<sub>2</sub> ratio on the C<sub>2</sub> selectivity at different temperature.

#### 4.3.2. Experiments with Different Catalysts Forms

Sodium, tungsten and manganese components of Mn/Na<sub>2</sub>WO<sub>4</sub>/SiO<sub>2</sub> play essential roles in achieving high CH<sub>4</sub> conversion and high C<sub>2</sub> hydrocarbon selectivity in the OCM reactions as proven with various studies. However, the studies suggest that further increase of CH<sub>4</sub> conversion and C<sub>2</sub> selectivity is unlikely if the searches are limited to the catalyst compositions; the effects of structural changes in catalysts and reactor should be also investigated to find more effective structures.

Various methods were used to obtain various structural forms of catalyst. For example sol-gel method gave a chance to embed the active metals in the catalyst pore while other active metal can be impregnated on the catalyst surface. It is also possible to get distinctive catalyst pore size by changing sol-gel parameters.

In this work, three particulate catalysts were sensitized using sol-gel method, direct hydrothermal synthesis method (MCM-41) and monosil (whole structural rod catalyst) via sol-gel method with adding PEG. Figure 4.7 shows the catalysts that are prepared by varied types of method.

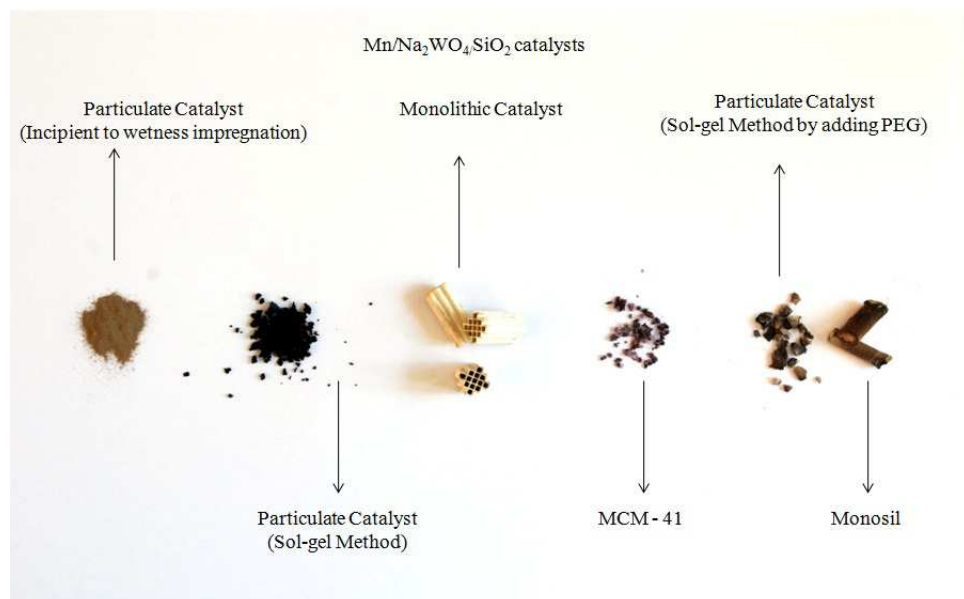


Figure 4.7. Various types of catalysts prepared via different methods.

A particulate catalyst was prepared by sol-gel method (without adding PEG) as mentioned in Section 3.2.1.2. The construction of the catalyst was weak and during the high temperature calcinations process, they were smashed. The catalyst was tested at 650 and 700°C reaction temperature at two CH<sub>4</sub>/O<sub>2</sub> ratios (7 and 10). The comparison between two temperatures and CH<sub>4</sub>/O<sub>2</sub> ratio are given in Table 4.1; C<sub>2</sub> selectivity increased 1-2% with increasing temperature and CH<sub>4</sub>/O<sub>2</sub> ratio while CH<sub>4</sub> conversion was stayed the same.

Table 4.2 indicates the catalytic performance of the particulate catalysts that were prepared by sol-gel method adding 4.79 gr. The catalyst showed nearly the same CH<sub>4</sub> conversion as the catalyst without PEG but the selectivity was much higher at 650°C temperature (it was about 42% in both CH<sub>4</sub>/O<sub>2</sub> ratios of 7 and 10).

Table 4.1. Particulate catalyst\* performance at temperature 650 and 700°C, CH<sub>4</sub>/O<sub>2</sub> ratio 7 and 10.

Temperature (°C)	CH <sub>4</sub> /O <sub>2</sub>	C <sub>2</sub> selectivity	CH <sub>4</sub> conversion
650	7	14.24	31.74
650	10	17.27	31.84
700	7	16.5	31.63
700	10	18.00	31.71

\*0.2 gr particulate catalyst was prepared by sol-gel method without addition of PEG.

Table 4.2. Particulate catalyst\* performance at temperature 650 and 700°C, CH<sub>4</sub>/O<sub>2</sub> ratio 7 and 10.

Temperature (°C)	CH <sub>4</sub> /O <sub>2</sub>	C <sub>2</sub> selectivity	CH <sub>4</sub> conversion
600	7	18.91	32.54
650	7	42.27	32.83
650	10	42.58	29.47

\*0.2 gr particulate catalyst was prepared by sol-gel method adding PEG.

The most important parameter for the strength of catalyst prepared was the amount of the PEG used. The experiments showed that high value of the PEG decrease the mechanical resistance. This was also reported by Nakanishi *et al.* (1998) and Martin *et al.* (2001) and attributed to the fact that the excess quantity of the PEG decreases the strength of the solid skeleton.

Table 4.3 and 4.4 show the catalytic performance of the catalysts that were prepared by sol-gel method adding 4 gr. PEG; the only difference between the catalysts used in two tables are that only Na<sub>2</sub>WO<sub>4</sub> was impregnated over the sol-gel prepared material containing Mn and all other ingredients in Table 4.3 while and Mn and Na<sub>2</sub>WO<sub>4</sub> were impregnated in

the catalyst in Table 4.4. The C<sub>2</sub> selectivity and CH<sub>4</sub> conversion rates did not change significantly.

Table 4.3. Monosil catalyst\* performance at temperature 650 and 700°C, CH<sub>4</sub>/O<sub>2</sub> ratio 7 and 10.

Temperature (°C)	CH <sub>4</sub> /O <sub>2</sub>	C <sub>2</sub> selectivity	CH <sub>4</sub> conversion
650	7	26.06	29.59
700	7	32.36	30.03
700	10	33.23	29.89

\*0.3 gr. Monosil catalyst is used, Mn is added via sol-gel method, Na<sub>2</sub>WO<sub>4</sub> was impregnated.

Table 4.4. Monosil catalyst performance at temperature 650 and 700°C, CH<sub>4</sub>/O<sub>2</sub> ratio 7 and 10.

Temperature (°C)	CH <sub>4</sub> /O <sub>2</sub>	C <sub>2</sub> selectivity	CH <sub>4</sub> conversion
650	7	26.15	29.46
650	10	27.87	31.70
700	7	30.43	30.08
700	10	32.03	31.86

\*0.3 gr. Monosil catalyst is used, Mn and Na<sub>2</sub>WO<sub>4</sub> were impregnated.

Research on the highly ordered pore structure lead to synthesize a mesoporous silica support called as MCM-41. The mesoporous structured catalyst was tested at the same reaction conditions and results are listed below at Table 4.5. It showed nearly the same CH<sub>4</sub> conversion when compared with the other catalyst form. The change of CH<sub>4</sub>/O<sub>2</sub> ratio from 7 to 10 caused only some minor improvement in selectivity.

Table 4.5. MCM-41 catalyst\* performance at temperature 650°C and 700°C, CH<sub>4</sub>/O<sub>2</sub> ratio 7 and 10.

Temperature (°C)	CH <sub>4</sub> /O <sub>2</sub>	C <sub>2</sub> selectivity	CH <sub>4</sub> conversion
650	7	26.15	29.45
650	10	27.87	31.70
700	7	30.43	30.03
700	10	32.03	31.86

\*0.2gr MCM-41 catalyst, Na<sub>2</sub>WO<sub>4</sub> was impregnated.

Table 4.6. Comparasion of the catalysts that are prepared by different methods (Reaction temperature at 700°C, CH<sub>4</sub>/O<sub>2</sub> ratio is 10).

Catalyst	C <sub>2</sub> selectivity	CH <sub>4</sub> conversion	Yield
Particulate catalyst (prepared by incipient to wetness impregnation)	45.86	30.95	14.19
Particulate catalyst (prepared by sol-gel method without PEG)	18.00	31.71	5.70
Particulate catalyst (prepared by sol-gel adding PEG)	42.58	29.47	12.54
Monosil catalyst	32.03	31.86	10.20
MCM-41 catalyst	32.03	31.86	10.21

The catalytic performances of the catalysts were prepared in various ways were summarized in Table 4.6 and Figure 4.7. Highest selectivity was achieved over the catalysts prepared by incipient to wetness impregnation, followed by the catalyst prepared by sol-gel method with PEG. A similar result was reported by Wang *et al.* (2006) that

catalyst (that was prepared by sol-gel) showed lower  $\text{CH}_4$  conversion and  $\text{C}_2\text{H}_4$  selectivity than prepared catalyst by incipient to wetness impregnation.

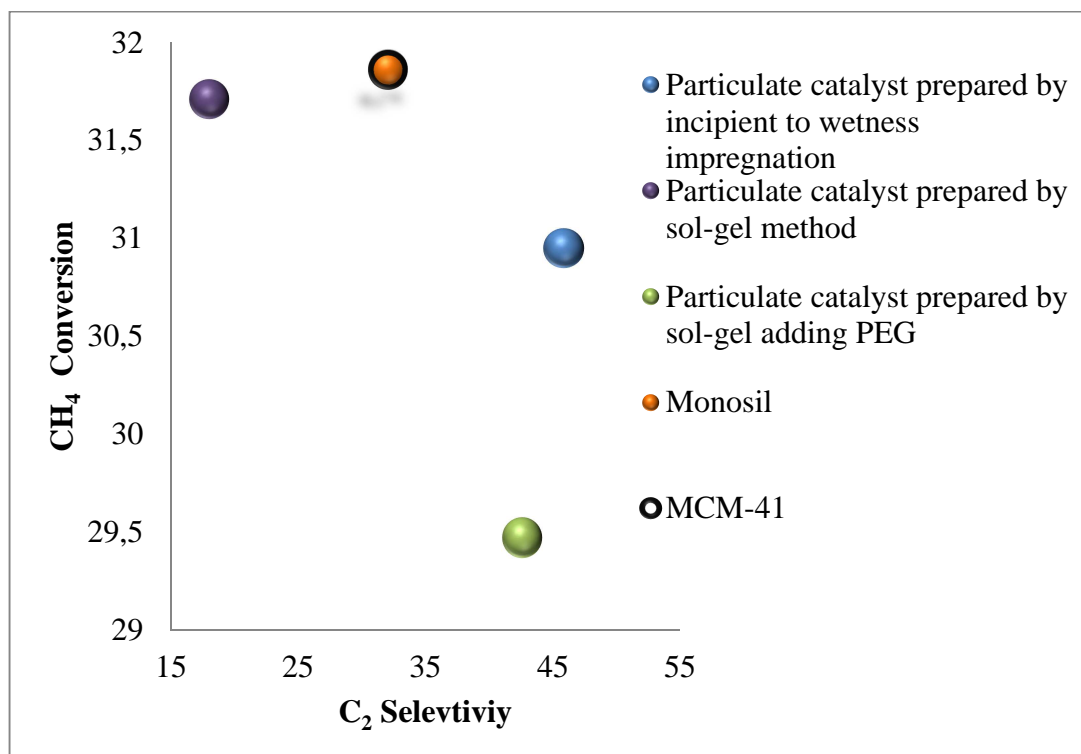


Figure 4.8. Comparison of the catalysts that are prepared by different methods (reaction temperature at  $700^\circ\text{C}$ ,  $\text{CH}_4/\text{O}_2$  ratio is 10).

The  $\text{CH}_4$  conversion and  $\text{C}_2$  selectivity were not changed significantly over various catalysts that were prepared using different procedures. Liu *et al.* (2008) reported similar results for 5wt.% $\text{Na}_2\text{WO}_4$ /2wt.%Mn/SiC monolithic foam catalyst. In their work, the active metals were impregnated in monolithic foam with the diameter 9 mm, length 20 mm with a pore (4.1 mm) in the middle along its axis. The catalyst performance was compared with the particulate catalyst that was prepared via incipient to wetness impregnation method. Both catalysts showed nearly same catalytic activity; highest  $\text{C}_2$  selectivity (52.7%) was achieved at  $850^\circ\text{C}$  with 16.8%  $\text{CH}_4$  conversion. Increasing temperature to  $900^\circ\text{C}$  showed negative effect on the  $\text{C}_2$  selectivity; it was reduced to 47%. It was pointed out that the catalyst not only showed the same catalytic performance but showed an excellent heat transfer feature.

## 5. CONCLUSIONS AND RECOMMENDATIONS

### 5.1. Conclusions

The aim of this study was to develop and test various alternative catalysts and reactor structures to improve the performance of 2wt.%Mn and 5wt.%Na<sub>2</sub>WO<sub>4</sub>catalyst for OCM reactions. The major conclusions that can be drawn from the study are as follows;

- Coated particulate Mn/Na<sub>2</sub>WO<sub>4</sub>/SiO<sub>2</sub> catalyst on the FeCrAl alloy plate showed the weak adhesion and mechanical resistance. The low C<sub>2</sub> yield was obtained in the micro-structured reactor tests.
- Monosil (whole structural rod catalyst) and MCM-41 mesoporous structured catalysts showed similar CH<sub>4</sub> conversion and C<sub>2</sub> selectivity at the same reaction operating conditions.
- Highest yield (14.2%) was obtained with the particulate catalyst that was prepared by incipient to wetness impregnation method. This is followed by the catalyst synthesized via sol-gel method addition of template material (12.5% yield).
- The quartz reactor inside diameter was decreased 10 mm to 2 mm initial diameter after the catalyst bed. This improved the C<sub>2</sub> selectivity significantly although it did not change the conversion.
- Filing the empty space in the quartz reactor volume with  $\alpha$ -Al<sub>2</sub>O<sub>3</sub> improved the selectivity and increasing the mesh size of the particles affects the yield positively. The quartz chips, however, were more suitable filling material. The pure crushed SiO<sub>2</sub> and quartz sand, on the other hand, did not work because they blocked the gas flow.
- The C<sub>2</sub> selectivity was maximized (55.8%) at the temperature of 650°C and CH<sub>4</sub>/O<sub>2</sub> ratio of 7.

## 5.2. Recommendations

According to the results of the present study, the following points are thought to be beneficial for the future studies;

- The length of the reactor can be minimized to reduce the contribution of gas phase reactions.
- The filling material can be changed and provided more homogenous contribution of filling in the reactor to improve the catalytic performance of the reactor.
- An alternative catalyst structure can be developed. The structure can be more stable than monosil and provide more sufficient heat transfer.
- A microstructured reactor can be developed, which consists of the silica structure and also includes microchannels.

## APPENDIX A: CALIBRATION CURVES OF MASS FLOW CONTROLLERS

Calibration curves of the mass flow controllers used in the experiments are illustrated below.

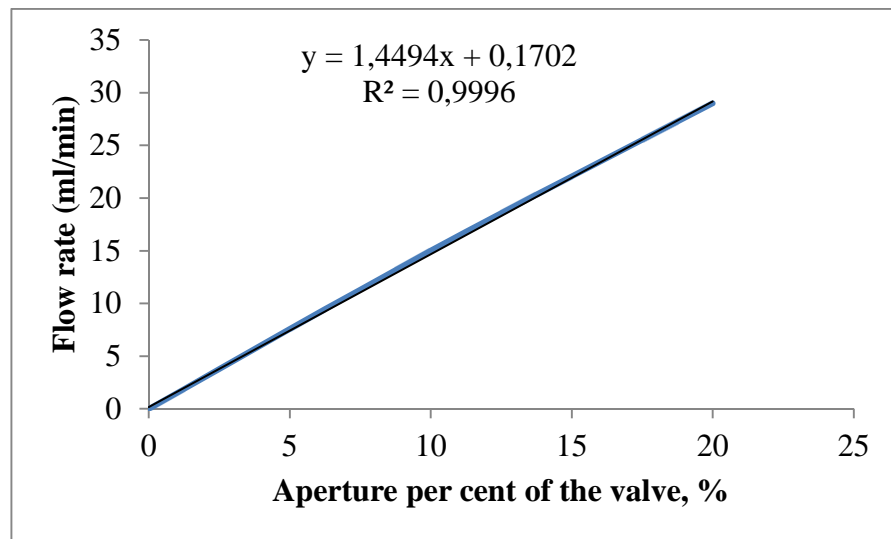


Figure A.1. MFC calibration curve for ethylene.

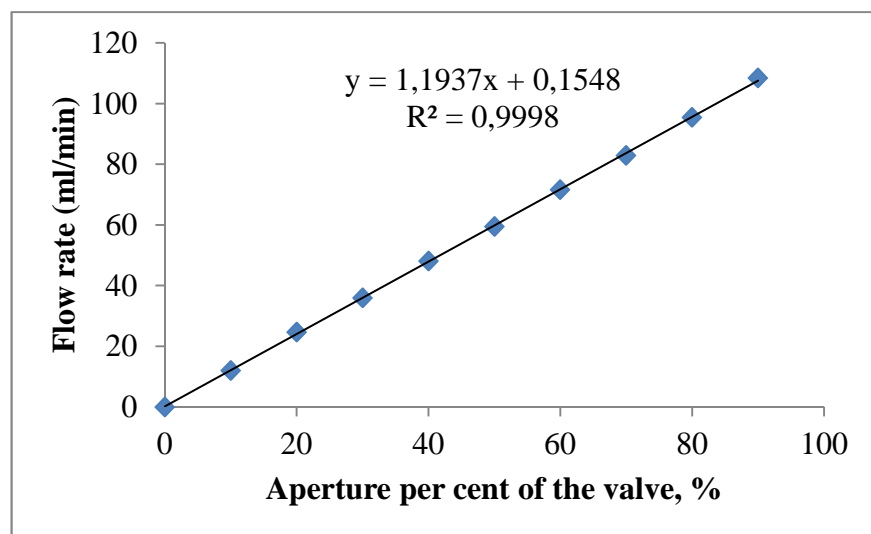


Figure A.2. MFC calibration curve for methane.

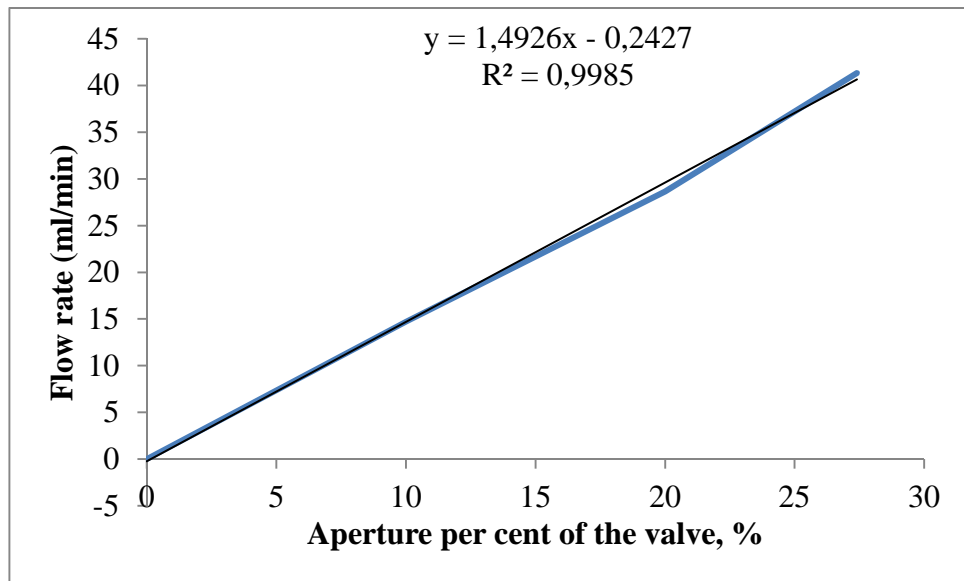


Figure A.3. MFC calibration curve for ethane.

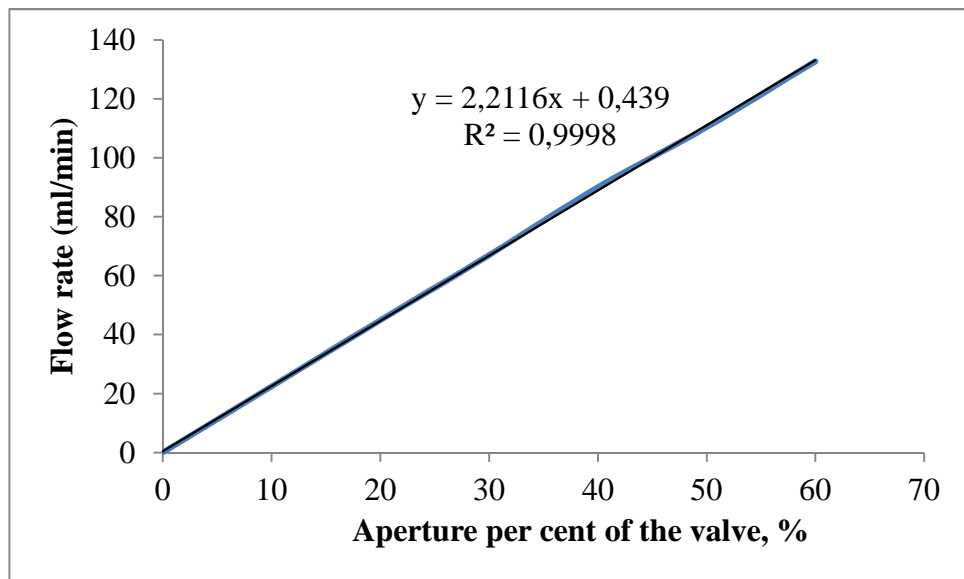


Figure A.4. MFC calibration curve for oxygen.

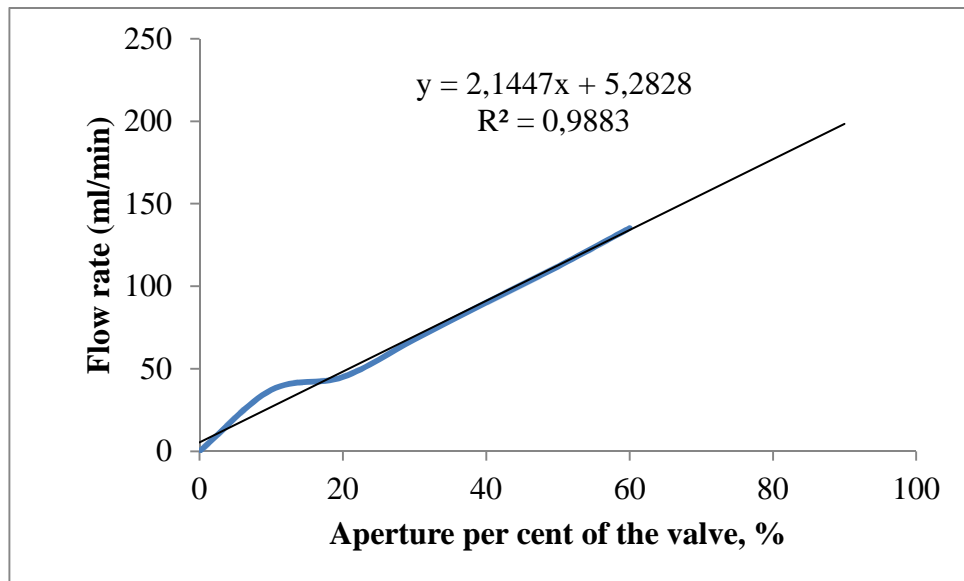


Figure A.5. MFC calibration curve for helium.

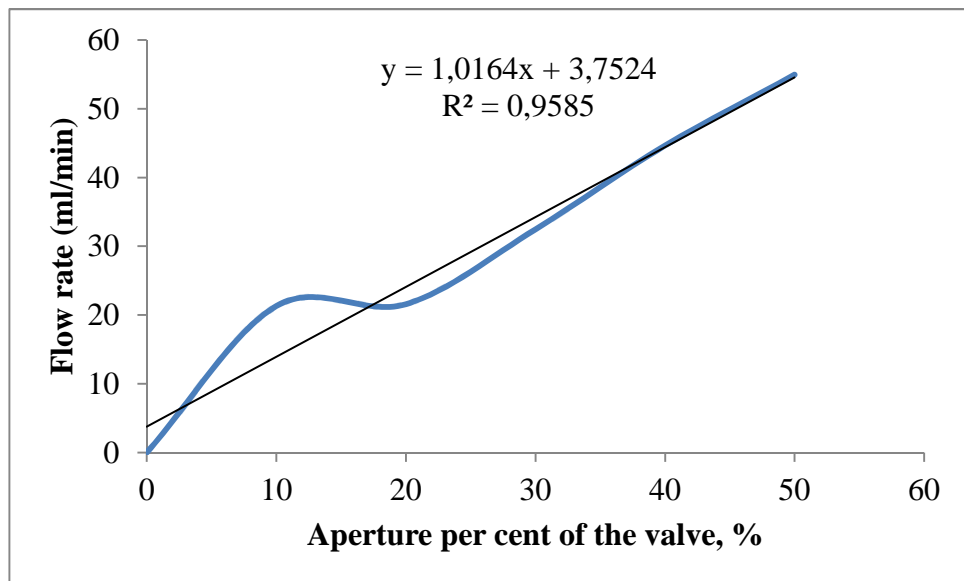


Figure A.6. MFC calibration curve for hydrogen.

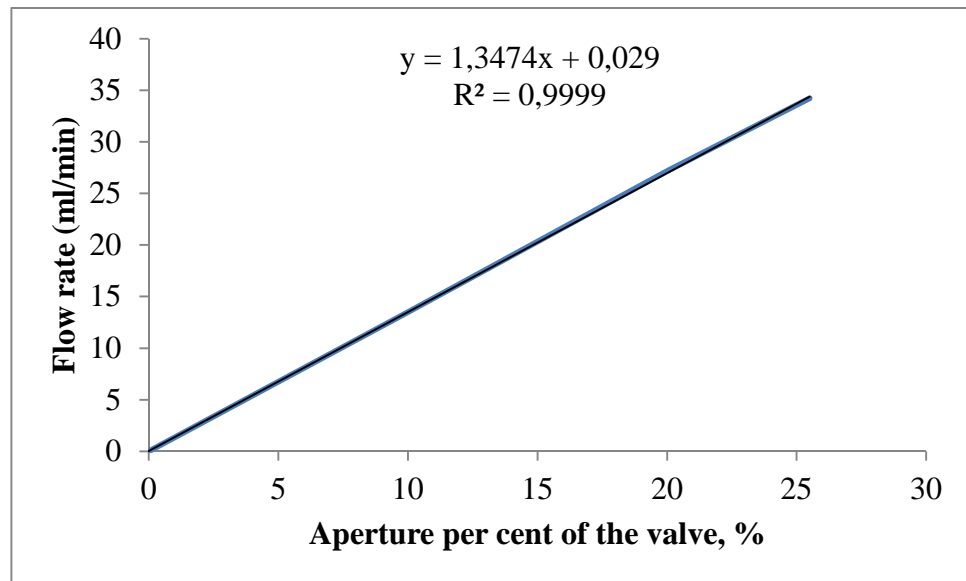


Figure A.7. MFC calibration curve for mixture (5% methane, 2% ethane, 2% ethylene, 81% helium).

## REFERENCES

- Akin, F. T. and Y. S. Lin, 2002, "Oxidative Coupling of Methane in Dense Ceramic", *AIChE Journal Membrane Reactor with High Yields*, Vol. 48, No. 10, pp. 2298-2306.
- Alvarez-Galvan, M. C., N. Mota, M. Ojeda, S. Rojas, R. M. Navarro and J. L. G. Fierro, 2011, "Direct Methane Conversion Routes to Chemicals and Fuels", *Catalysis Today*, Vol. 171, No. 63, pp. 15-23.
- Au, C. T., Y. W. Liu, and C. F. Ng, 1998, "Raman Spectroscopic and TPR Studies of Oxygen Species Over BaO and BaX<sub>2</sub> (X = F, Cl, Br)-Promoted Nd<sub>2</sub>O<sub>3</sub> Catalysts for the Oxidative Coupling of Methane", *Journal Catalysis*, Vol. 176, No. 11, pp. 365-375.
- Aartun, I., H. J. Venvik, A. Holmen, P. Pfeifer, O. Görke and K. Schubert, 2004, "Temperature Profiles and Residence Time Effects During Catalytic Partial Oxidation and Oxidative Steam Reforming of Propane in Metallic Microchannel Reactors", *Catalysis Today*, Vol. 110, pp. 98-107.
- Baerns, M., D. Schweer and L. Meeckol, 1990, "Oxidative Coupling of Methane: Maximizing the Yield of Coupling Products Under Co-feed Operating Conditions", *Catalysis Today*, Vol. 6, pp. 453-462.
- Cameron, G., L. Le, J. Levine and N. Nagulapalli, 2012, "*Process Design for the Production of Ethylene from Ethanol*", Design Project, University of Pennsylvania.
- Chou, L., Y. Cai, B. Zhang, J. Nio, S. Ji and S. Li., 2003, "Influence of SnO<sub>2</sub>-doped W-Mn/SiO<sub>2</sub> for Oxidative Coupling of Methane to High Hydrocarbons at Elevated Pressure", *Applied Catalysis A*, Vol. 238, pp. 185-191.

- Choudhary, V. R., S. B. S. Uphade, and S. A. R. Mulla, 1997, "Oxidative Coupling of Methane over a Sr-Promoted  $\text{La}_2\text{O}_3$  Catalyst Supported on a Low Surface Area Porous Catalyst Carrier", *Industrial and Engineering Chemistry Research*, Vol. 36, pp. 3594-3601.
- Choudhary, V. R., S. A. R. Mulla and B. S. Uphade, 1999, "Oxidative Coupling of Methane Over Alkaline Earth Oxides Deposited on Commercial Support Precoated with Rare Earth Oxides", *Fuel*, Vol. 78, No. 4, pp. 427-437.
- Choudhary, V. R. and B. S. Uphade, 2004, "Oxidative Conversion of Methane/Natural Gas Into Higher Hydrocarbons", *Catalysis Surveys from Asia*, Vol. 8, No. 1, pp. 15-25.
- Doğu, T., S. Balci and Y. Gucbilmez, 2005, "Vanadium Incorporated High Surface Area MCM-41 Catalysts", *Catalysis Today*, Vol. 100, pp. 473-477.
- Elkins, T. W. and H. E. Hagelin-Weaver, 2013, "Oxidative Coupling of Methane Over Unsupported and Alumina-Supported Samaria Catalysts", *Applied Catalysis A: General*, Vol. 454, pp. 100-114.
- Gomez, R., T. Lopez, P. Bosch, J. Navarette and M. Asomoza, 1994, "Structure of Pd/ $\text{SiO}_2$  Sol-gel and Impregnated Catalysts", *Journal of Sol-gel Science and Technology*, Vol. 1, pp. 193-203.
- Fang, X. P., S. B. Li, H. L. Wang, Z. C. Jiang and C. J. Yu, "Oxide/Support Interaction and Surface Reconstruction in the Sodium Tungstate ( $\text{Na}_2\text{WO}_4$ )/Silica System", *The Journal of Physical Chemistry*, Vol. 97, No. 49, pp. 12870-12875.
- Fogler, H. S., 1992, "Elements of Chemical Reaction Engineering", Second Ed., *Prentice-Hall International Series of The Physical and Chemical Engineering Sciences*, pp.128.

- Gong, M. C., X. H. Xu, Y. Q. Chen, J. L. Zhou and Y. Chen, 1995, "Study on Oxidative Coupling of Methane Effect of Additives on TiO<sub>2</sub>-Based Catalytic Performance", *Catalysis Today*, Vol. 24, pp. 263-264.
- He, Y., B. Yang and G. Cheng, 2004, "On the Oxidative Coupling of Methane with Carbon dioxide Over CeO<sub>2</sub>/ZnO Nanocatalysts", *Catalysis Today*, Vol. 98, pp. 595-600.
- Hessel, V., K. Jähnisch, H. Löwe and M. Baerns, 2004, *Chemistry in Microstructured Reactors*, Angewandte Chemie International Edition, Vol. 43, No. 4, pp. 406-46.
- Holmen, A., 2009, "Direct Conversion of Methane to Fuels and Chemicals", *Catalysis Today*, Vol. 142, pp. 2-8.
- Ishizuka, N., H. Kobayashi, H. Minakuchi, K. Nakanishi, K. Hirao, K. Hosoya, T. Ikegami and N. Tanaka, 2002, "Monolithic Silica Columns for High-Efficiency Separations by High-Performance Liquid Chromatography", *Journal of Chromatography: A*, Vol. 960, pp. 85-96.
- Jašo, S., H. R. Godini, H. Arellano-Garcia and G. Wozny, 2010, "Oxidative Coupling of Methane: Reactor Performance and Operating Conditions", *Computer Aided Chemical Engineering*, Vol. 28, pp. 781-786.
- Ji, S., C. Li, W. Wang and D. Pan, 2011, "A Novel Particle/Monolithic Two-Stage Catalyst Bed Reactor and Their Catalytic Performance for Oxidative Coupling of Methane", *Fuel Processing Technology*, Vol. 92, pp. 541-546.
- Ji, S., T. Xiao, S. Li, L. Chou, B. Zhang, C. Xu, R. Hou and A. P. E. York, M. L. H. Green, 2003, "Surface WO<sub>4</sub> tetrahedron: the essence of the oxidative coupling of methane over M-W-Mn/SiO<sub>2</sub> catalysts", *Journal of Catalysis*, Vol. 220, pp. 47-56.
- Ji, S., T. Xiao, S. Li, C. Xu, R. Hou, K. S. Coleman and M.L.H. Green, 2002, "The Relationship Between The Structure and The Performance of Na-W-Mn/SiO<sub>2</sub>

- Catalysts for The Oxidative Coupling of Methane", *Applied Catalysis*, Vol. 225, pp. 271-284.
- Jiang, Z. C., C. J. Yu, X. P. Fang, S. B. Li and H. L. Wang, 1993, "Oxide/Support Interaction and Surface Reconstruction in The Sodium Tungstate( $\text{Na}_2\text{WO}_4$ )/Silica System", *The Journal of Physical Chemistry*, Vol. 97, pp. 12870-12875.
- Jing-jing, T., J. Sheng-fu, W. Kai and L. Cheng-yue, 2009, "Preparation of M-W-Mn/ $\text{SiO}_2$ /Cordierite Monolithic Catalysts and Their Performances for Oxidative Coupling of Methane", *Natural Gas Chemical Industry*, Vol. 3.
- Karimi, A., R. Ahmadi, H. R. Bozorg Zadeh, A. Jibreili Jolodar and A. Barkhordarion, 2007, "Catalytic Oxidative Coupling Of Methane - Experimental Investigation and Optimization Of Operational Conditions", *Petroleum and Coal*, Vol. 49, pp.36-40.
- Kataoka, S., Endo A., M. Oyama and T. Ohmori, 2009, "Enzymatic Reaction Inside a Microreactor with a Mesoporous Silica Catalyst Support Layer", *Applied Catalysis A: General*, Vol. 359, pp. 108-112.
- Keller, G. E. and M. M. Bhasin, 1982, "Synthesis of Ethylene via Oxidative Coupling of Methane", *Journal Catalysis*, Vol. 73, pp. 9-19.
- Kılavuz E., "Endüstriyel, Test ve Ölçü Cihazları", 2013, <http://www.ekilavuz.com>, accessed at April 2013.
- Kirschning, A., C. Altwicker, G. Dräger, J. Harders, N. Hoffmann, U. Hoffmann, H. Schönfeld, W. Solodenko and U. Kunz, 2001, *Pass Flow Syntheses Using Functionalized Monolithic Polymer/Glass Composites in Flow-Through Microreactors*, *Angewandte Chemie International Edition*, Vol. 40, pp. 3995-3998.
- Ko, E. I. and Edited by G. Ertl, H. Knözinger and J. Weitkamp, 1999, "Preperation of Solid Catalysts, Wiley-VCH", *Weinheim*, pp.85-98.

- Kolb, G. and V. Hessel, 2004, "Micro-Structured Reactors for Gas Phase Reactions", *Chemical Engineering Journal*, Vol. 98, pp.1-38.
- Kou, Y., B. Zhang, J. Niu, S. Li and H. Wang, 1998, "Amorphous Features of Working Catalysts: XAFS and XPS Characterization of Mn/Na<sub>2</sub>WO<sub>4</sub>/SiO<sub>2</sub> as Used for the Oxidative Coupling of Methane", *Journal of Catalysis*, Vol. 173, pp. 399-408.
- Lambert, C. K. and R. D. Gonzalez, 1998, "The Importance of Measuring the Metal Content of Supported Metal Catalysts Prepared by the Sol-Gel Method", *Applied Catalysis A: General*, Vol. 172, pp. 233-239.
- Lee, M. R., M. J. Park, W. Jeon, J.-W. Choi, Y.-W. Suh and D. J. Suh, 2012, "A Kinetic Model for the Oxidative Coupling of Methane over Na<sub>2</sub>WO<sub>4</sub>/Mn/SiO<sub>2</sub>", *Fuel Processing Technology*, Vol. 96, pp. 175-182.
- Li, S., J. Wang, L. Chou, B. Zhang, H. Song, J. Zhao and J. Yang, 2006, "Comparative Study on Oxidation of Methane to Ethane and Ethylene Over Na<sub>2</sub>WO<sub>4</sub>-Mn/SiO<sub>2</sub> Catalysts Prepared by Different Methods", *Journal of Molecular Catalysis A: Chemical*, Vol. 245, pp. 272-277.
- Li, S., 2003, "Reaction Chemistry of W-Mn/SiO<sub>2</sub> Catalyst for the Oxidative Coupling of Methane", *Journal of Natural Gas Chemistry*, Vol. 12, pp. 1-9.
- Li, S., S. Ji, T. Xiao, C. Xu, R. Hou, K. S. Coleman and M. L.H. Green, 2002, "The Relationship Between the Structure and the Performance of Na-W-Mn/SiO<sub>2</sub> Catalysts for the Oxidative Coupling of Methane", *Applied Catalysis*, Vol. 225, pp. 271-284.
- Liu, H., X. Wang, D. Yang, R. Gao, L. Chen and S. Zhang, 2008, "A Novel Na<sub>2</sub>WO<sub>4</sub>-Mn/SiC Monolithic Foam Catalyst with Improved Thermal Properties for the Oxidative Coupling of Methane", *Catalysis Communications*, Vol. 9, pp. 1302-1306.

- Lu, Y., A. G. Dixon, W. R. Moser, Y. H. Ma and U. Balachandran, 2000, "Oxygen-Permeable Dense Membrane Reactor For The Oxidative Coupling of Methane", *Journal of Membrane Science*, Vol. 170, pp. 27-34.
- Lunsford, J. H., 2000, "Catalytic Conversion of Methane to More Useful Chemicals and Fuels: A Challenge for the 21st Century", *Catalysis Today*, Vol. 63, pp. 165-174.
- Malekzadeh, A., A. K. Dalai, A. Khodadadi and Y. Mortazavi, 2007, "Structural Features of  $\text{Na}_2\text{WO}_4\text{-MO}_x/\text{SiO}_2$  Catalysts in Oxidative Coupling of Methane Reaction", *Catalysis Communications*, Vol. 9, pp. 960-965.
- Martin, J., B. Hosticka, C. Lattimer and P. M. Norris, 2001, "Mechanical and Acoustical Properties as a Function of PEG Concentration in Macroporous Silica Gels", *Journal of Non-Crystalline Solids*, Vol. 288, pp. 222.
- Mo, X., J. Gao and J. G. Goodwin Jr., 2009, "Role of Promoters on Rh/SiO<sub>2</sub> in CO Hydrogenation: A Comparison Using DRIFTS", *Catalysis Today*, Vol. 147, pp. 139-149.
- Nakanishi, K., H. Minakuchi, N. Soga and N. Tanaka, 1998, "Structure Design of Double-Pore Silica and Its Application to HPLC", *Journal of Sol-Gel Science and Technology*, Vol. 13, pp 163-169.
- Onsan, Z. I., 2007, "Catalytic Processes for Clean Hydrogen Production from Hydrocarbons", *Turkish Journal of Chemistry*, Vol. 31, pp. 531-550.
- Oshima, K., K. Tanaka, T. Yabe and E. Kikuchi, 2013, "Oxidative Coupling of Methane Using Carbondioxide in an Electric Field Over La-ZrO<sub>2</sub> Catalyst at Low External Temperature", *Fuel*, Vol. 107, pp. 879-881.
- Özdemir, C., 2006, *Low Temperature CO Oxidation in Hydrogen-Rich Streams Over Pt-SnO<sub>2</sub>/Al<sub>2</sub>O<sub>3</sub> Catalysts Prepared by Sol-Gel Method*, M. S. Thesis, Bogaziçi University, Istanbul.

- Özdemir, S., 2009, *Selective CO Oxidation Over Monolithic Au/Al<sub>2</sub>O<sub>3</sub> Promoted by Metal Oxides*, M. S. Thesis, Bogaziçi University, Istanbul.
- Palermo, A., J. P. Vazquez, A. F. Lee, S. Mintcho, R. M. Lambertz and T. Lambert, 1998, “Critical Influence of the Amorphous Silica-to-Cristobalite Phase Transition on the Performance of Mn/Na<sub>2</sub>WO<sub>4</sub>/SiO<sub>2</sub> Catalysts for the Oxidative Coupling of Methane”, *Journal of Catalysis*, Vol. 177, pp. 259-266.
- Perez-Cadenas, A. F., M. M. P. Zieverink, F. Kapteijn and J. A. Moulijn, 2005, “High Performance Monolithic Catalysts for Hydrogenation Reactions”, *Catalysis Today*, Vol., pp. 623-628.
- Perrichon, V., M. C. Durupty, 1988, “Thermal Stability of Alkali Metals Deposited on Oxide Supports and Their Influence on the Surface Area of the Support”, *Journal Catalysis*, Vol. 42, pp. 217-227.
- Rahimpour, M. R., M. R. Dehnavi, F. Allahgholipour, D. Iranshahi and S. M. Jokar, 2011, “Assessment and Comparison of Different Catalytic Coupling Exothermic and Endothermic Reactions: A review”, *Applied Catalysis*, Vol. 99, pp. 496-512.
- Sachse, A., V. Hulea, A. Finiels, B. Coq, F. Fajula and A. Galarneau, 2012, “Alumina-grafted Macro-/Mesoporous Silica Monoliths as Continuous Flow Microreactors for The Diels–Alder Reaction”, *Journal of Catalysis*, Vol. 287, pp. 62-67.
- Sachse, A., A. El Kadib, R. Chimenton, F. Fajula, A. Galarneau and B. Coq, 2009, “Functionalized Inorganic Monolithic Microreactors for High Productivity in Fine Chemicals Catalytic Synthesis”, *Journal of Catalysis*, Vol. 48, pp. 4969-4972.
- Sergei, P., Q. Ping and J. H. Lunsford, 1998, “Elementary Reactions in the Oxidative Coupling of Methane over Mn/Na<sub>2</sub>WO<sub>4</sub>/SiO<sub>2</sub> and Mn/Na<sub>2</sub>WO<sub>4</sub>/MgO Catalysts”, *Journal of Catalysis*, Vol. 179, pp. 222-230.

- Simsek, E., 2012, *Catalytic Synthesis Gas Production in Microchannel Reactors*, Ph. D. Thesis, Bogaziçi University, Istanbul.
- Siouffi, A. M., 2003, "Silica Gel-Based Monoliths Prepared by the Sol-Gel Method: Facts and Figures", *Journal of Chromatography: A*, Vol. 1000, pp. 801-818.
- Sofranko, J. A., J. J. Leonard and C. A. Jones, 1987, "Oxidative Coupling of Methane over Oxide-Supported Sodium-Manganese Catalysts", *Journal of Catalysis*, Vol. 155, pp. 390-402.
- Somayeh, M. and E. Mohammad Reza, 2011, "Effect of Additives on Mn/SiO<sub>2</sub> Based Catalystson Oxidative Coupling of Methane", *Iranian Journal of Chemistry and Chemical Engineering*, Vol. 30, No.1.
- Swaan, H. M., Y. Li, K. Seshan, J.G. Van Ommen and J. R. H. Ross, 1993, "The Oxidative Coupling of Methane and the Oxidative Dehydrogenation of Ethane Over a Niobium Promoted Lithium Doped Magnesium Oxide Catalyst", *Catalysis Today*, Vol. 16, pp. 537-546.
- Talebizadeh, A., V. Salehoun, A. Khodadadi and Y. Mortazavi, 2008, "Dynamics of Mn/Na<sub>2</sub>WO<sub>4</sub>/SiO<sub>2</sub> Catalyst in Oxidative Coupling of Methane", *Chemical Engineering Science*, Vol. 63, pp. 4910-4916.
- Talebizadeh, A., Y. Mortazavi and A. A. Khodadadi, 2009, "Comparative Study of The Two-Zone Fluidized-bed Reactor and The Fluidized-bed Reactor for Oxidative Coupling of Methane Over Mn/Na<sub>2</sub>WO<sub>4</sub>/SiO<sub>2</sub> Catalyst", *Fuel Processing Technology*, Vol. 90, pp. 1319-1325.
- Talebizadeh, A., M. Daneshpayeh, A. Khodadadi, N. Mostoufi, Y. Mortazavi and R. Sotudeh-Gharebagh, 2009, "Kinetic Modeling of Oxidative Coupling of Methane Over Mn/Na<sub>2</sub>WO<sub>4</sub>/SiO<sub>2</sub> Catalyst", *Fuel Processing Technology*, Vol. 90, pp. 403-410.

Thackeray, F., “Turning Natural Gas Into Diesel Has Many Advantages, Especially in the US”, 2013, <http://www.petroleum-economist.com/Article/3160595/GTL-pushes-at-the-margins.html>, accessed at April 2013.

Tiemersma, T. P., M. J. Tuinier, F. Gallucci, J. A. M. Kuipers and M. van Sint Annaland, “2012, “A Kinetics Study for the Oxidative Coupling of Methane on a Mn/Na<sub>2</sub>WO<sub>4</sub>/SiO<sub>2</sub>Catalyst”, *Applied Catalysis A: General*, Vol. 433-434 , pp. 96-108.

Tomastic, V. and F. Jovic, 2006, “State-of-the-art in the Monolithic Catalysts/Reactors”, *Applied Catalysis A: General*, Vol. 311, pp. 112-121.

Tye, C. T., A. R. Mohamed and S. Bhatia, 2002, “Modeling of Catalytic Reactor for Oxidative Coupling of Methane Using La<sub>2</sub>O<sub>3</sub>/CaO Catalyst”, *Chemical Engineering Journal*, Vol. 87, pp. 49-59.

Vasireddy, S., S. Ganguly, J. Sauer, W. Cook and J. J Spivey, 2011, “Direct Conversion of Methane to Higher Hydrocarbons Using AlBr<sub>3</sub>-HBr Superacid Catalyst”, *The Royal Society of Chemistry*, Vol.47, pp.785-787.

Yoğurtçu, B., 2012, *An Experimental Study On The Effect Of Metal Loading On WGS Performance Of Au-Re System*, Ph. D. Thesis, Bogaziçi University, Istanbul.

Young, S. K., “Sol-Gel Science for Ceramic Materials”, 2006, <http://www.sigmaaldrich.com/technical-documents/articles/material-matters/sol-gel-science-for.html>, accessed at April 2013.

Zhang, L., D. Chen and Y. Liu, 2012, “Vertical and In-situ Growth of Hexaaluminate Embedded in Alumina Intermediate Layer with High Stability”, *The Royal Society of Chemistry*, Vol.3, pp.2534.

- Wang, D. J., M. P. Rosynek and J. H. Lunsford, 1995, "Oxidative Coupling of Methane over Oxide-Supported Sodium-Manganese Catalysts", *Journal of Catalysis*, Vol. 155, pp. 390-402.
- Wang, J., L. Chou, B. Zhang, H. Song, J. Zhao, J. Yang and S. Li, 2005, "Comparative Study on Oxidation of Methane to Ethane and Ethylene Over  $\text{Na}_2\text{WO}_4\text{-Mn/SiO}_2$  Catalysts Prepared by Different Methods", *Journal of Molecular Catalysis A: Chemical*, Vol. 245, pp. 272-277.
- Wang, J., L. Chou, B. Zhang, H. Song, J. Yang, J. Zhao and S. Li, 2006, "Low-Temperature Selective Oxidation of Methane to Ethane and Ethylene Over  $\text{BaCO}_3/\text{La}_2\text{O}_3$  Catalysts Prepared by Urea Combustion Method", *Catalysis Communications*, Vol. 7, pp. 59-63.
- Wolf, E. E., 1992, "Methane Conversion by Oxidative Processes: Fundamental and Engineering Aspects", Van Nostrand Reinhold, New York.